Electronic topological defect dynamics in metastable states: from forced to quantum

Dragan Mihailovic
Jozef Stefan Institute, Ljubljana, Slovenia, Univ. of Ljubljana, CENN Nanocenter

22/2/2022

Image: Quantum jamming of electrons (Nat. Mat. 2019)


Jaka Vodeb
Jan Ravnik
Polona Aupič (expt)
Yaroslav Gerasimenko
Emil Bozin, BNL
Michele Diegox
Tomaz Mertelj
Rok Venturini
Igor Vaskivskyi
Yevhenii Vaskivskyi
Denis Golež
Viktor Kabanov
Peter Karpov
Serguei Brazovskii
Yelizaveta Chernolevska
Anze Mraz

Life exists (only) out of equilibrium

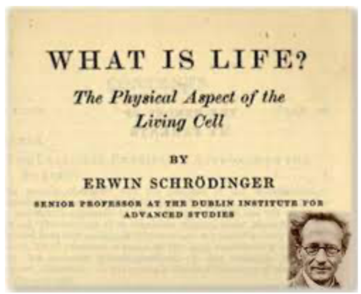

Edwin Schroedinger, What is life? (1944)

Protein folding bottlenecks (metastability – first order phase transitions)

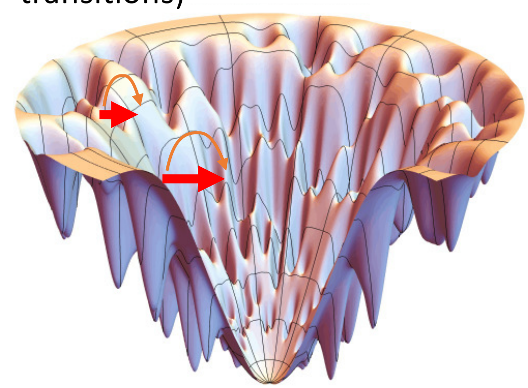

The standard model

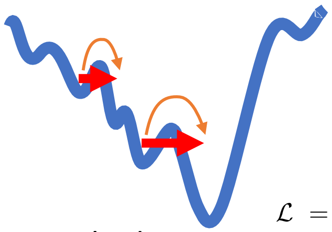

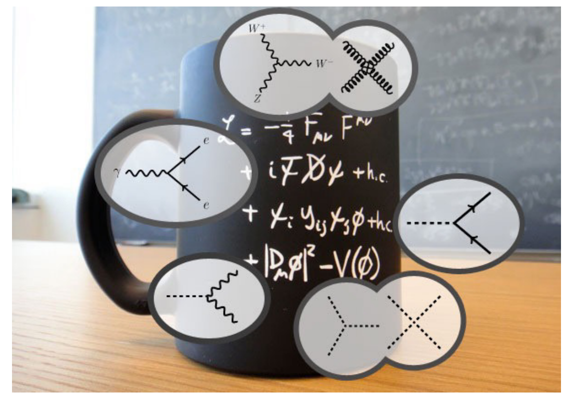

$$\begin{aligned}
\mathcal{L} = & -\frac{1}{4}B_{\mu\nu}B^{\mu\nu} - \frac{1}{8}tr(\mathbf{W}_{\mu\nu}\mathbf{W}^{\mu\nu}) - \frac{1}{2}tr(\mathbf{G}_{\mu\nu}\mathbf{G}^{\mu\nu}) && \text{(U(1), SU(2) and SU(3) gauge terms)} \\
& +(\bar{\nu}_L, \bar{e}_L)\,\tilde{\sigma}^\mu iD_\mu \begin{pmatrix}\nu_L \\ e_L\end{pmatrix} + \bar{e}_R\sigma^\mu iD_\mu e_R + \bar{\nu}_R\sigma^\mu iD_\mu \nu_R + \text{(h.c.)} && \text{(lepton dynamical term)} \\
& -\frac{\sqrt{2}}{v}\left[(\bar{\nu}_L, \bar{e}_L)\,\phi M^e e_R + \bar{e}_R\bar{M}^e\bar{\phi}\begin{pmatrix}\nu_L \\ e_L\end{pmatrix}\right] && \text{(electron, muon, tauon mass term)} \\
& -\frac{\sqrt{2}}{v}\left[(-\bar{e}_L, \bar{\nu}_L)\,\phi^* M^\nu \nu_R + \bar{\nu}_R\bar{M}^\nu\phi^T\begin{pmatrix}-e_L \\ \nu_L\end{pmatrix}\right] && \text{(neutrino mass term)} \\
& +(\bar{u}_L, \bar{d}_L)\,\tilde{\sigma}^\mu iD_\mu \begin{pmatrix}u_L \\ d_L\end{pmatrix} + \bar{u}_R\sigma^\mu iD_\mu u_R + \bar{d}_R\sigma^\mu iD_\mu d_R + \text{(h.c.)} && \text{(quark dynamical term)} \\
& -\frac{\sqrt{2}}{v}\left[(\bar{u}_L, \bar{d}_L)\,\phi M^d d_R + \bar{d}_R\bar{M}^d\bar{\phi}\begin{pmatrix}u_L \\ d_L\end{pmatrix}\right] && \text{(down, strange, bottom mass term)} \\
& -\frac{\sqrt{2}}{v}\left[(-\bar{d}_L, \bar{u}_L)\,\phi^* M^u u_R + \bar{u}_R\bar{M}^u\phi^T\begin{pmatrix}-d_L \\ u_L\end{pmatrix}\right] && \text{(up, charmed, top mass term)} \\
& +\overline{(D_\mu\phi)}D^\mu\phi - m_h^2[\bar{\phi}\phi - v^2/2]^2/2v^2. && \text{(Higgs dynamical and mass term)}
\end{aligned}$$

(

Causality and the dynamics of emergent orders after a 2^{nd} order PT

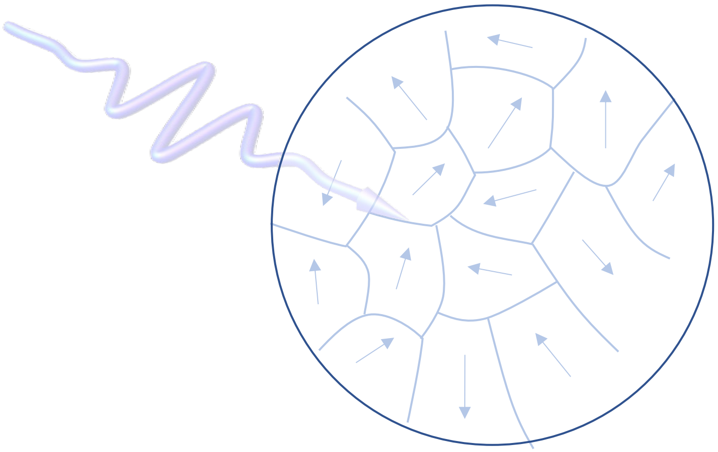

System size: laser spot, universe, etc.

The Kibble-Zurek Mechanism

$$\tau_{quench} \sim \left(\frac{dT}{dt}\right)^{-1} T_c$$

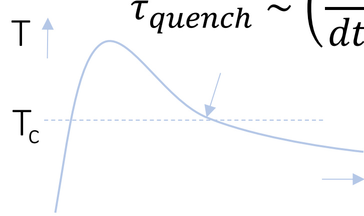

The picture is naïve, assuming a common temperature, no interactions, etc.

Control of the outcome:

Tempering of steel:
Control of defects and domains

- Tempering of system trajectories can controllably lead to different transition outcomes
- CONTROL KNOBS: spatial and temporal gradients, transient strain, tailored laser pulse sequences, etc.

T. Kibble, J Phys a-Math Gen **9**, 1387 (1976).
W. Zurek, Nature **317**, 505 (1985).

Possible single transition outcomes

Starobinsky – Linde – Guth
Kibble, Zurek, Volovik

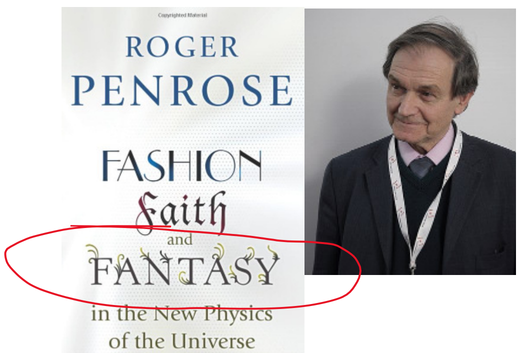

Figure: Roger Penrose's 'Fantasy'

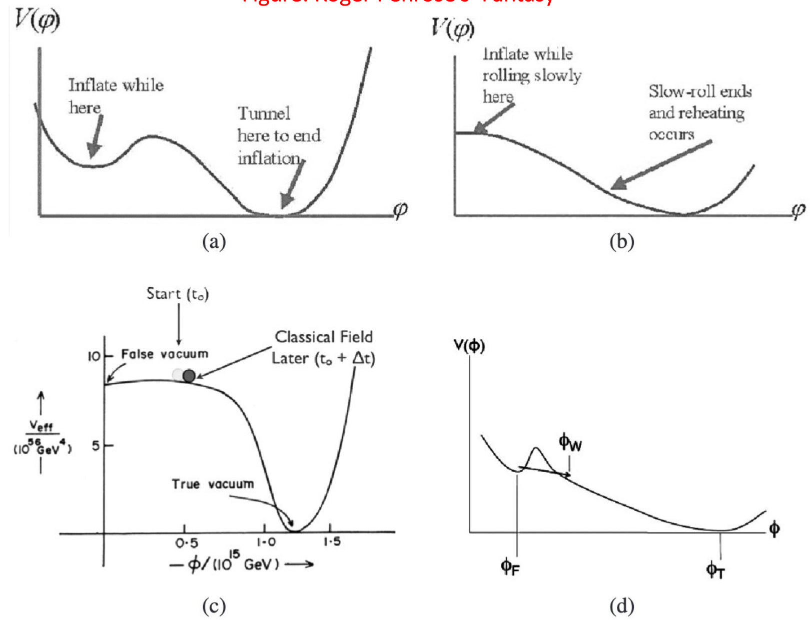

We have little data over a vast range of timescales!

Techniques for studying metastable, aperiodic, mesoscopic quantum structures

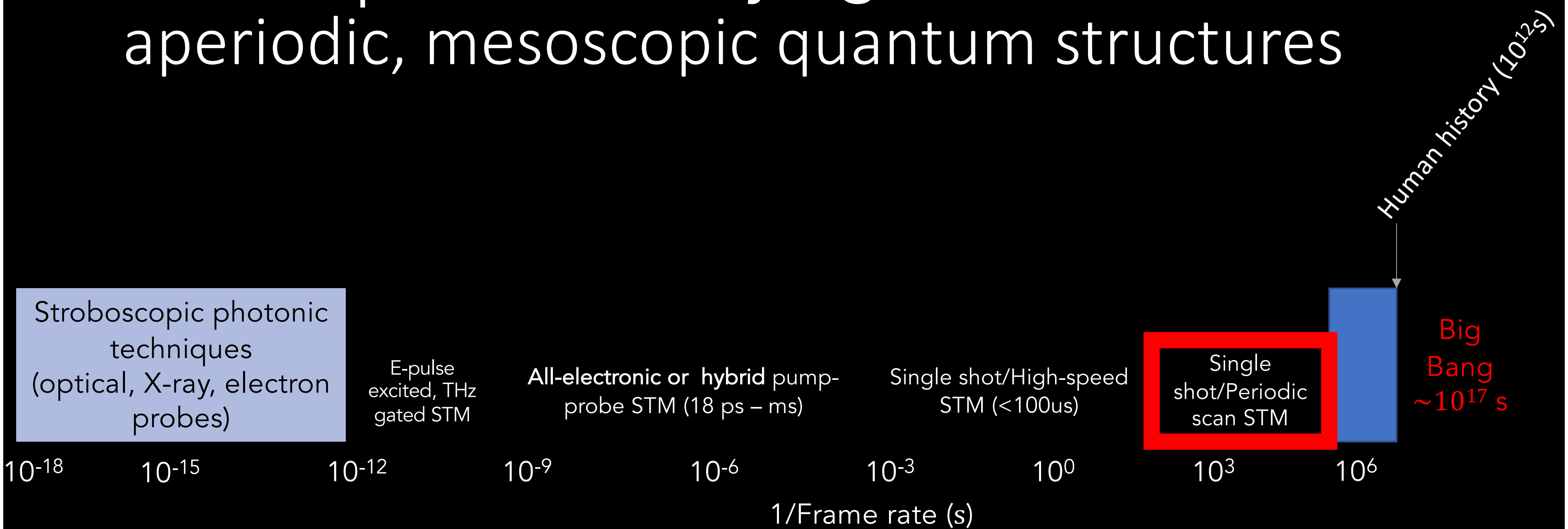

1T-TaS_2 as a prototype system

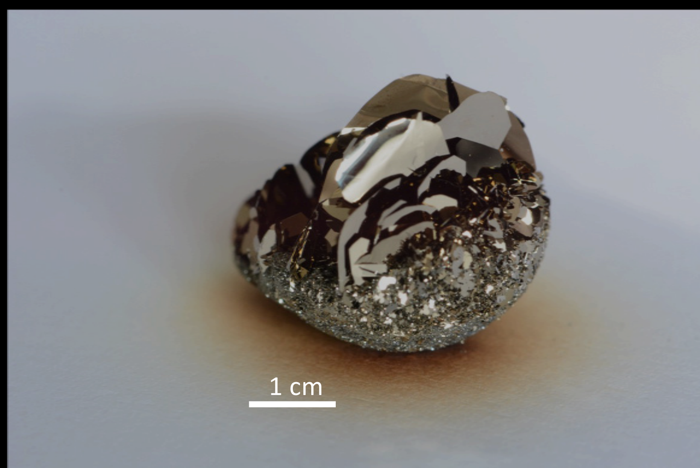

Crystals of 1T-TaS_2 grown by Petra Sutar

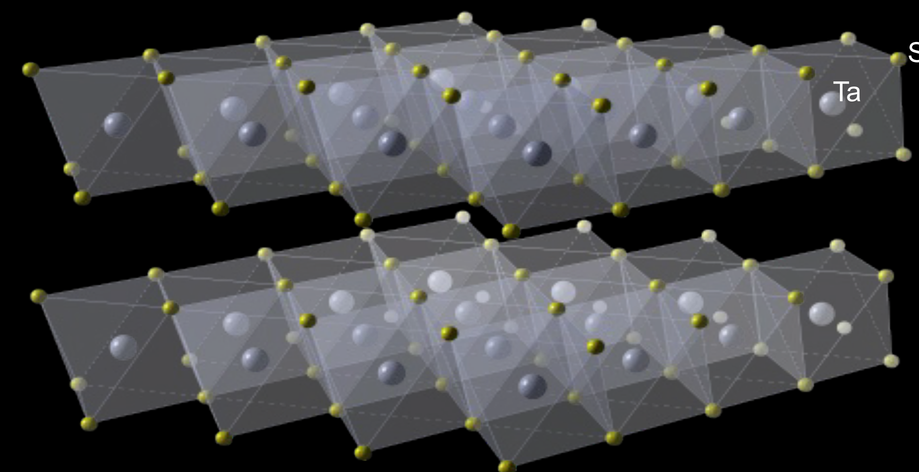

The threshold for localization, as defined by the dimensionless parameter, $r_s = \frac{V}{T} = \frac{e^2 m^*}{\hbar^2 \sqrt{n}} \sim 30$ **in 2D.**

1T-TaS_2 , with $m^* \sim 3 - 5m_e \rightarrow \mathrm{r_s} = \frac{V}{t} = 70 \sim 100$, is in the Wigner crystal regime

Controllable metastable states in *1T*-TaS_2

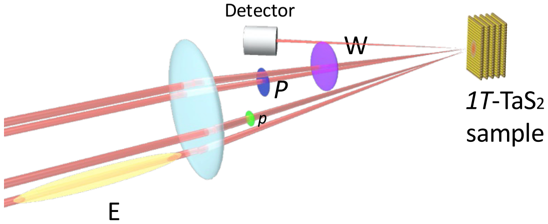

W = 50 fs "write"
E = 50 ps "erase"
P = "pump" (50 fs)
p = "probe" (50 fs)

Ljupka Stojchevska

Igor Vaskivskyi

CDW Collective mode frequency switching

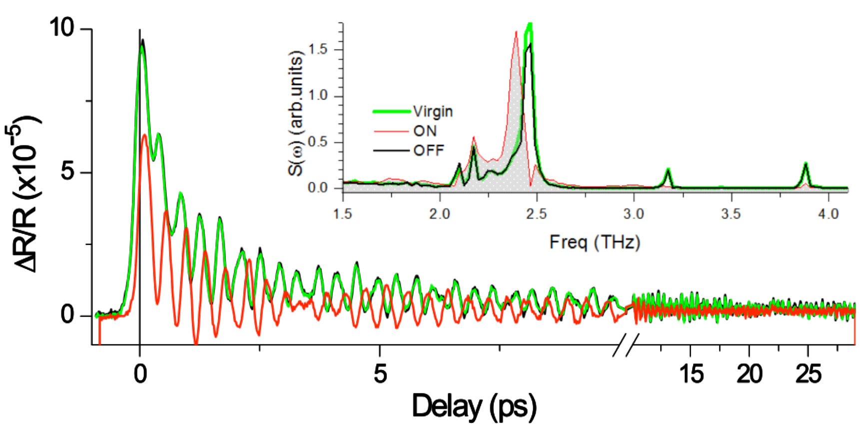

Resistance change after a (single) 35 fs pulse

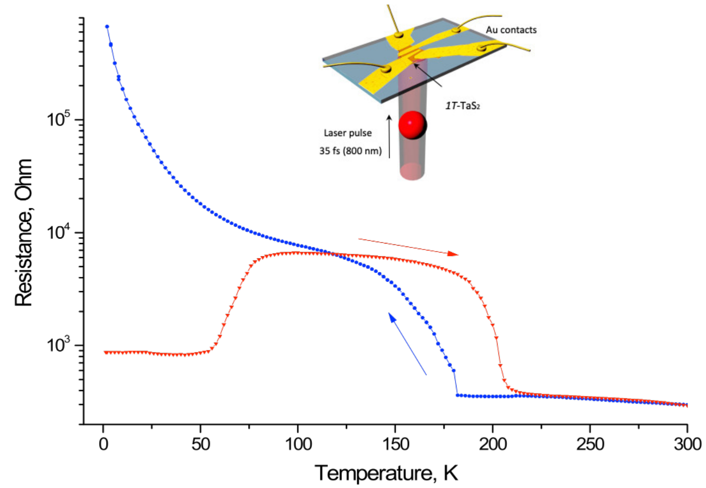

L Stojchevska et al. Science 2014;344:177-180

EMERGING TRECHNOLOGY

Charge Configuration Memory (CCM)

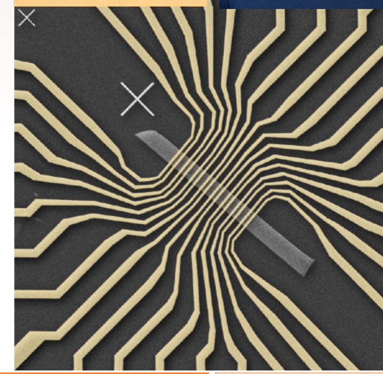

AN 2-TERMINAL ULTRAFAST ELECTRONIC NON-VOLATILE MEMORY CONCEPT FOR LOW-TEMPERATURE, ULTRA HIGH SPEED, LOW-ENERGY APPLICATIONS.

NANO LETTERS
pubs.acs.org/NanoLett Letter

Charge Configuration Memory Devices: Energy Efficiency and Switching Speed

Anze Mraz,* Rok Venturini, Damjan Svetin, Vitomir Sever, Ian Aleksander Mihailovic, Igor Vaskivskyi, Bojan Ambrozic, Goran Dražić, Maria D'Antuono, Daniela Stornaiuolo, Francesco Tafuri, Dimitrios Kazazis, Jan Ravnik, Yasin Ekinci, and Dragan Mihailovic

Cite This: https://doi.org/10.1021/acs.nanolett.2c01116 Read Online

Applied Physics Letters ARTICLE scitation.org/journal/apl

Ultrafast non-thermal and thermal switching in charge configuration memory devices based on 1T-TaS_2

Cite as: Appl. Phys. Lett. **119**, 013106 (2021); doi: 10.1063/5.0052311
Submitted: 30 March 2021 · Accepted: 31 May 2021 ·
Published Online: 8 July 2021

D. Mihailovic,[1,2,a)] D. Svetin,[1,2] I. Vaskivskyi,[1,2] R. Venturini,[1,4] B. Lipovšek,[3] and A. Mraz[1,3]

Applied Physics Letters ARTICLE scitation.org/journal/apl

Ultraefficient resistance switching between charge ordered phases in 1T-TaS_2 with a single picosecond electrical pulse

Cite as: Appl. Phys. Lett. **120**, 000000 (2022); doi: 10.1063/5.0096850
Submitted: 22 April 2022 · Accepted: 14 June 2022 ·
Published Online: 0 Month 0000

Rok Venturini,[1,2,a)] Anže Mraz,[1,3] Igor Vaskivskyi,[1] Yevhenii Vaskivskyi,[1,2] Damjan Svetin,[1,4] Tomaž Mertelj,[1] Leon Pavlovič,[5] Jing Cheng,[6] Genyu Chen,[6] Priyanthi Amarasinghe,[7] Syed B. Qadri,[8] Sudhir B. Trivedi,[7] Roman Sobolewski,[6,9] and Dragan Mihailovic[1,4,a)]

Institut "Jožef Stefan" Ljubljana, Slovenija

COSYLAB CONTROL SYSTEM LABORATORY

PAUL SCHERRER INSTITUT PSI

HYPRES The Digital Superconductor Company™

Nanocenter

Ultra-fast, ultra-efficient cryo-memory

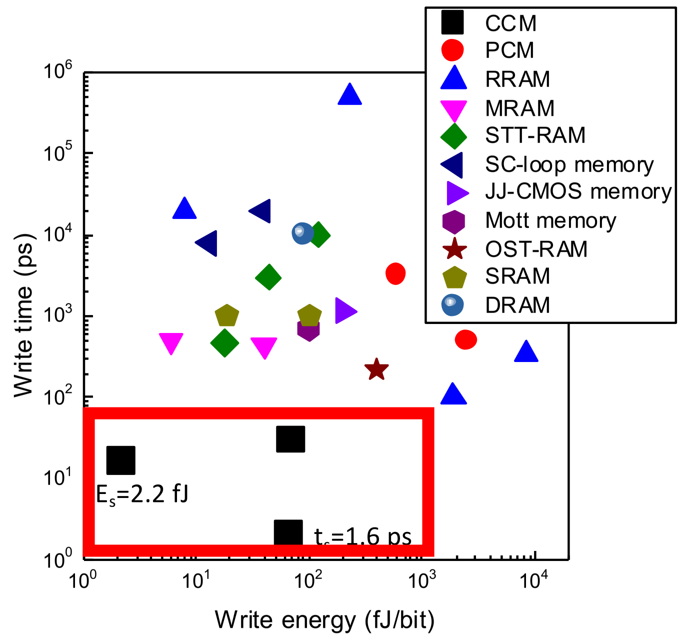

Mihailovic et al, APL, 2021, Venturini et al, APL, 2022

Hybrid CCM-nTron (pTron) memory

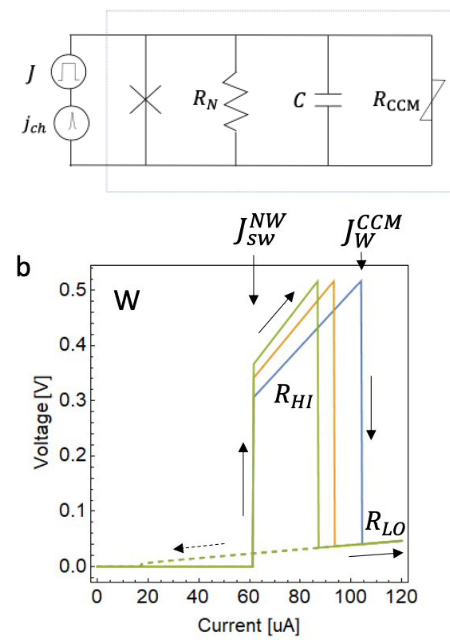

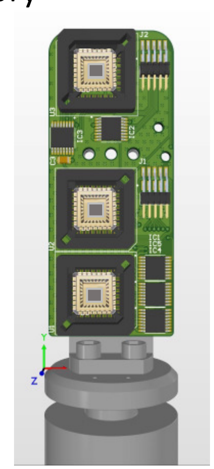

Institut "Jožef Stefan" Ljubljana, Slovenija

PAUL SCHERRER INSTITUT PSI

Nanocenter

Multiple US pats.

$1T$-TaS_2 under equilibrium conditions

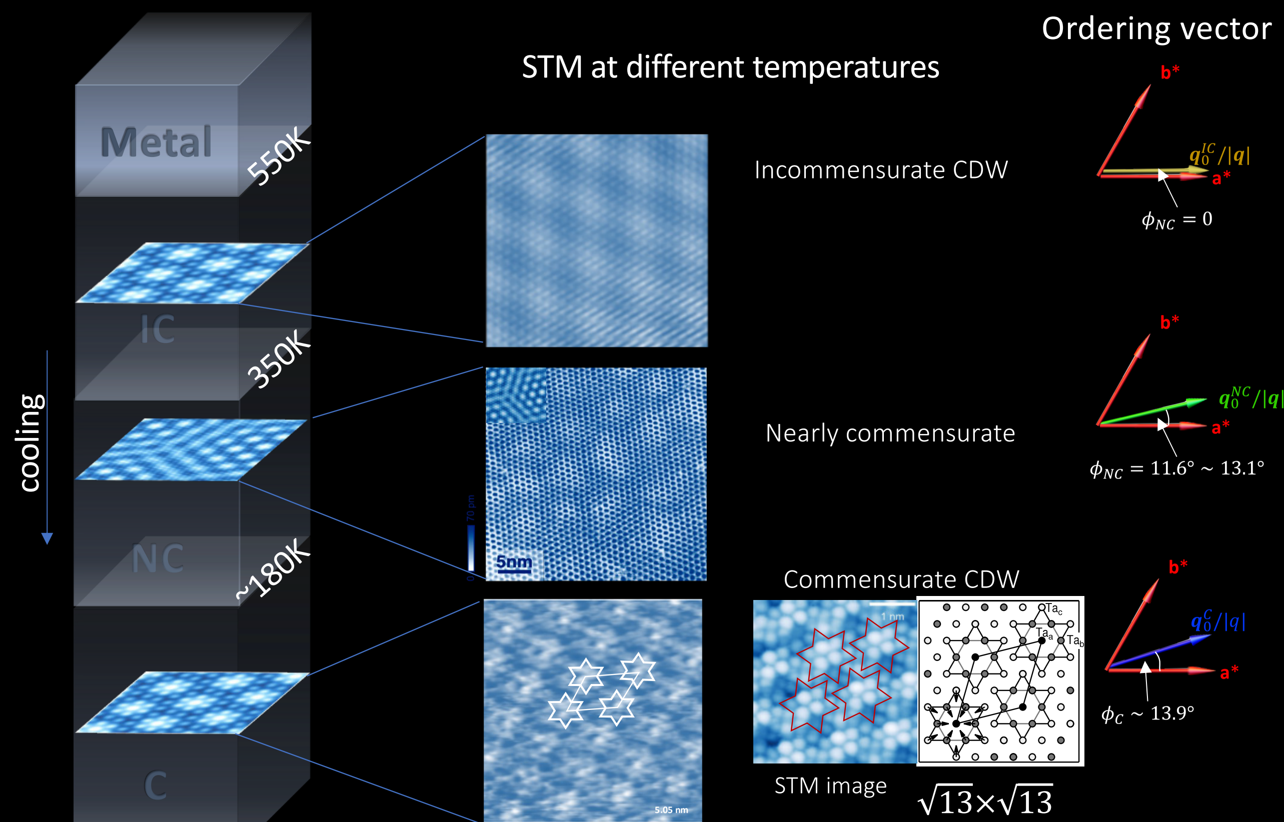

A Wigner crystal of polarons

Structural X-ray PDF study
10K - 600K

Chiral Ta displacements

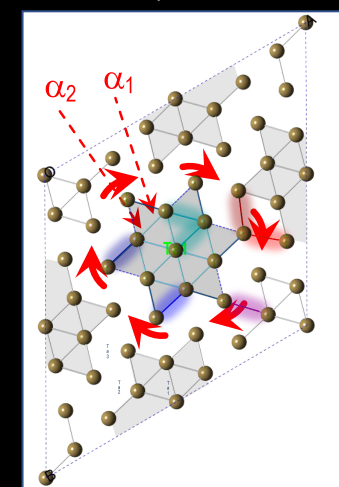

Emil Bozin, BNL
2022, to be published

The many phases in TaS_2: Multiple structural and charge-density-wave states, superconductivity under pressure, and/or (Fe,Cu,Na or Se…?) doping.

The 1T polytype of TaS_2 is metastable ($T_{c\uparrow}$=550K, $T_{c\downarrow}$=1100K)

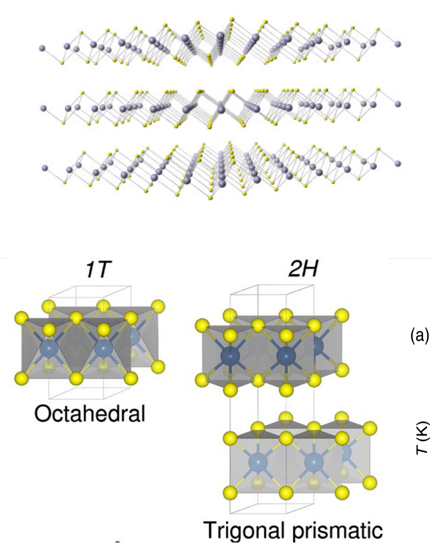

Fe : 1T-TaS_2

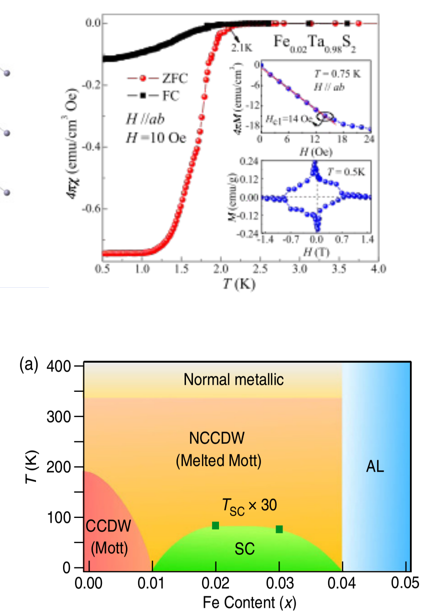

Li et al. EPL 2012

Cu : 2H-TaS_2

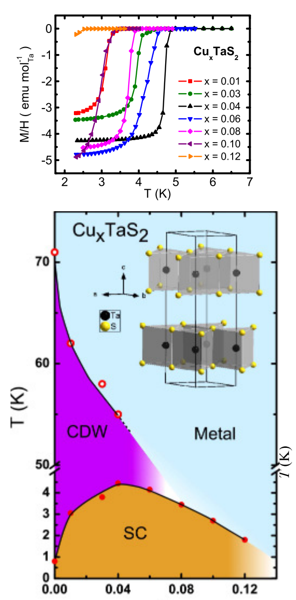

Wagner et al (PRBB 2008)

1T-$TaS_{2-x}Se_x$:

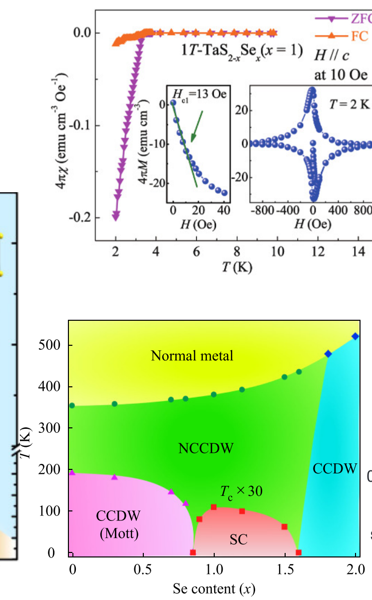

Liu et al. APL 2013

Pressure: 1T-TaS_2

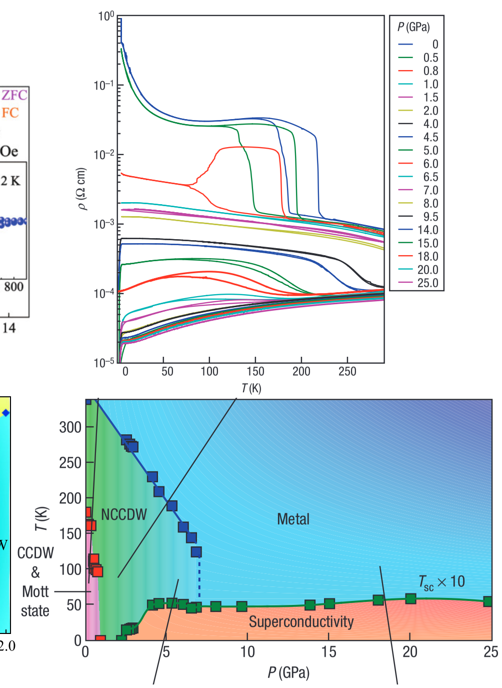

Sipos et al (Nat.Mat. 2008)

The ‘quantum spin liquid’ state of 1T-TaS_2

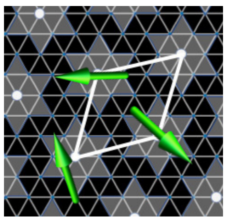

$\sqrt{13}\times\sqrt{13}$ superlattice

Charge gap $0.3 \sim 0.4\ eV$

ARPES

Hellmann et al, Nat. Comm. 2012

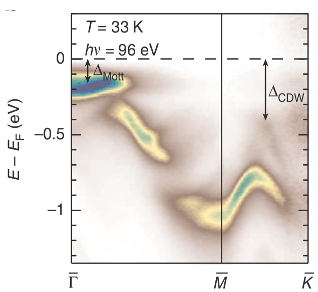

STM

Gerasimenko, 2017

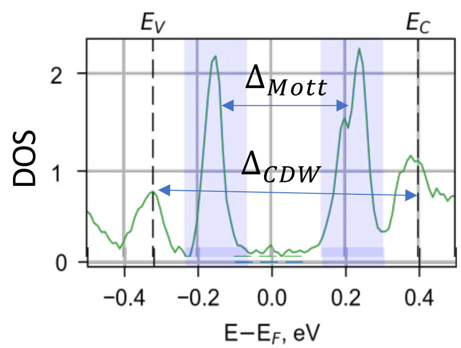

nature physics ARTICLES
PUBLISHED ONLINE: 31 JULY 2017 | DOI: 10.1038/NPHYS4212

A high-temperature quantum spin liquid with polaron spins

Martin Klanjšek[1], Andrej Zorko[1], Rok Žitko[1], Jernej Mravlje[1], Zvonko Jagličić[2,3], Pabitra Kumar Biswas[4], Peter Prelovšek[1,5], Dragan Mihailovic[1,5] and Denis Arčon[1,5]*

NQR Spin relaxation is gaples 50~180K! ($1\backslash T_1 \sim T^2$)

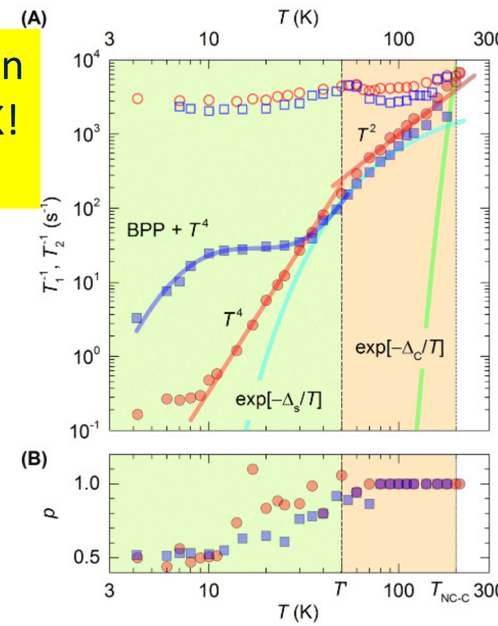

The workhorse: a time-resolved 4-probe STM/SEM microscope.

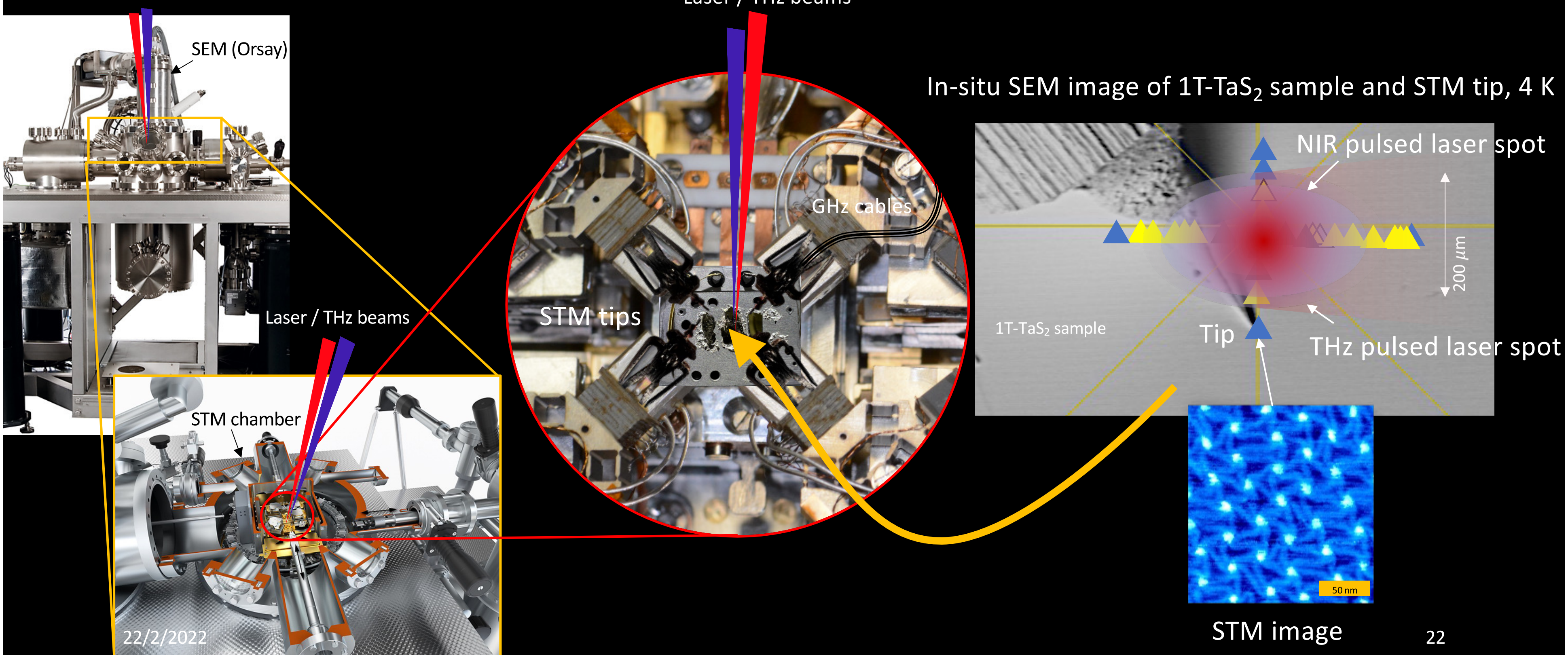

A time-domain phase diagram in 1T-TaS_2

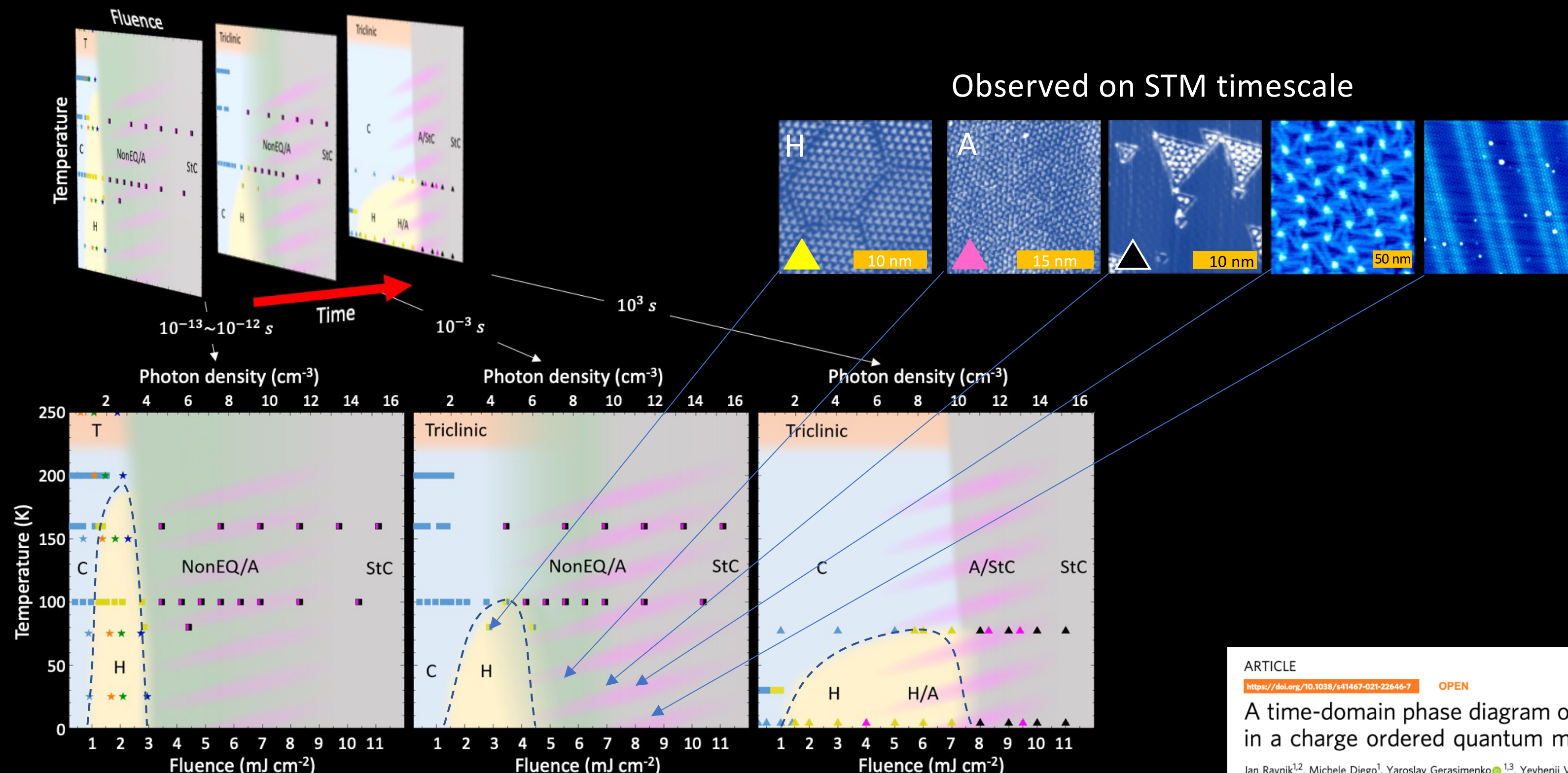

ARTICLE
https://doi.org/10.1038/s41467-021-22646-7 OPEN

A time-domain phase diagram of metastable states in a charge ordered quantum material

Jan Ravnik[1,2], Michele Diego[1], Yaroslav Gerasimenko[1,3], Yevhenii Vaskivskyi[1], Igor Vaskivskyi[1,3], Tomaz Mertelj[1,3], Jaka Vodeb[1] & Dragan Mihailovic[1,3,4]✉

NATURE COMMUNICATIONS | (2021)12:2323 |

The problem of characterizing metastable states that evolve during measurements

Jacques Henri Lartigue, 1913
(4x5 Speed Graphic camera with focal plane shutter)

Commensurate CDWs in dichalcogenides as polaronic Wigner crystals* ($r_s = V/t \sim 70$)

Sparse electron ordering on a triangular lattice

1/3

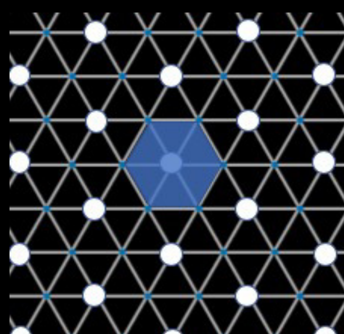

1/4

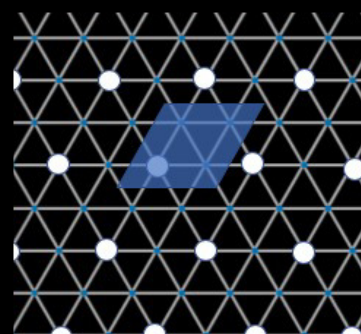

1/13

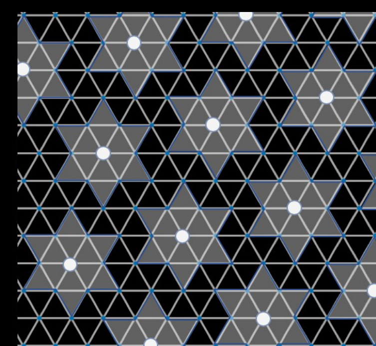

- Vodeb, J. *et al.* *New J Phys* **21,** 083001–16 (2019).
- Drummond and Needs, Phys. Rev. Lett. (2009)
- Camjayi,, Haule, Dobrosavljević & Kotliar, *Nat Phys* **4,** 932–935 (2008).

* a Mott-Wigner-polaronic state in 1T-TaS_2

SCIENTIFIC REPORTS

OPEN

: 23 November 2017

Modeling of networks and globules of charged domain walls observed in pump and pulse induced states

Petr Karpov[1] & Serguei Brazovskii[1,2,3]

Charged lattice gas model with only Coulomb interactions

$$H = \sum_{i,j} U_{ij} n_i n_j ,$$

Thomas-Fermi screening:

$$U_{ij} = e^2 \frac{\exp(-r/l_s)}{|\mathbf{r}_i - \mathbf{r}_j|} ;$$

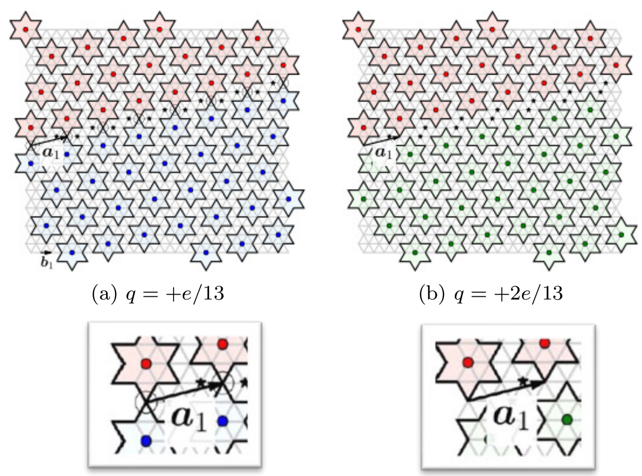

(a) $q = +e/13$ (b) $q = +2e/13$

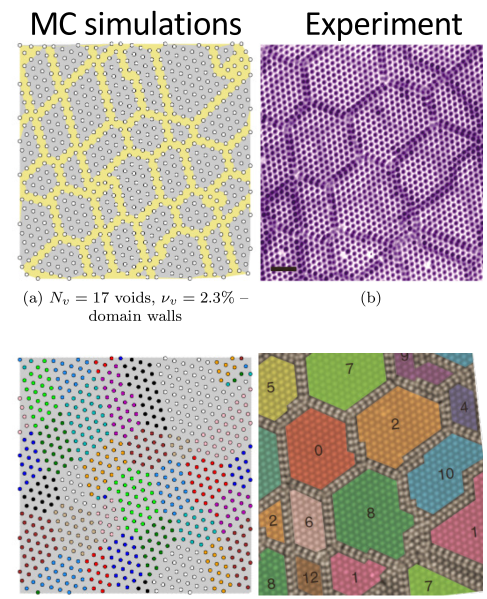

(a) $N_v = 17$ voids, $\nu_v = 2.3\%$ – domain walls (b)

(c) $N_v = 17$ voids, $\nu_v = 2.3\%$ (d)

Karpov, P. & Brazovskii, S. *Sci Rep* **8,** 1–7 (2018).

MC simulation of Polaronic Wigner crystals

Magic filling fractions lead to ordered Wigner crystalline phases

Charged lattice gas model with screened coulomb interaction:

$$\mathcal{H} = \sum_{i<j} V(i,j) n_i n_j,$$

where

$$V(i,j) = V_0 \frac{\exp(-r_{ij}/r_s)}{r_{ij}}$$

Hole-doped

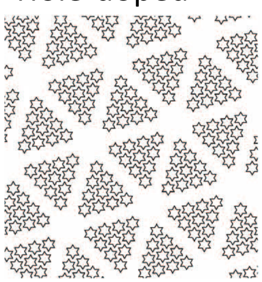

Stojchevska et al., Science (2014)

Electron-doped

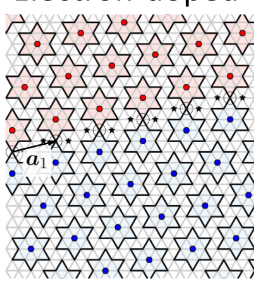

Karpov & Brazovskii. Sci Rep (2018).

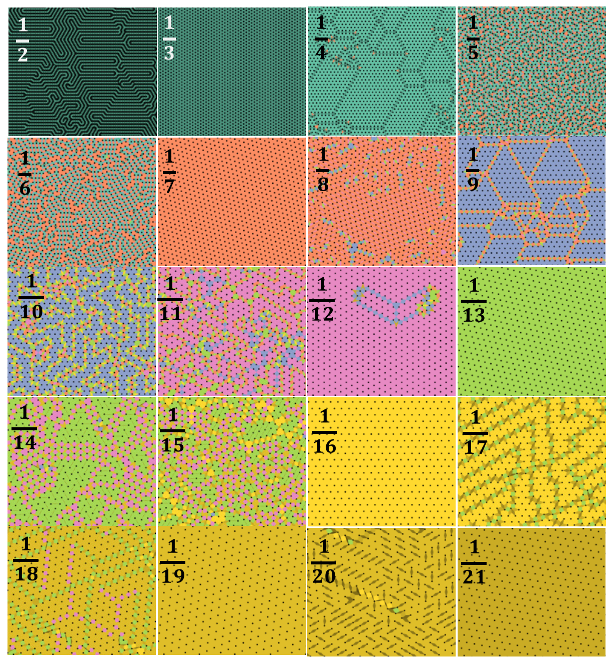

System	f	Phase
2H-$Fe_{0.33}TaS_2$	1/3	crystal
1T-$TiSe_2$	1/4	crystal
1T-$Cu_{0.08}TiSe_2$	1/4.2	domain state
2H-$Fe_{0.33}TaSe_2$	1/4	crystal
2H-$Fe_{0.33}NbSe_2$	1/4	crystal
2H-TaS_2	1/9	crystal
2H-$TaSe_2$	1/9	crystal
2H-$NbSe_2$	$\sim 1/9$	domain state
1T-TaS_2	1/13	crystal
PD 1T-TaS_2	1/12.6	domain state
1T-TaSeS	1/12.6	domain state
1T-$Ta_{0.99}Fe_{0.01}S_2$	1/12.6	domain state
1T-$Nb_{0.04}TaS_2$	$\sim 1/13$	domain state
1T-$Nb_{0.07}TaS_2$	$\sim 1/13$	domain state
PD 1T-TaS_2	1/11	amorphous state
1T-$Nb_{0.1}TaS_2$	$\sim 1/11$	possible amorphous state
4Hb-TaS_2	1/13	crystal
1T-$TaSe_2$	1/13	crystal
1T-$Ti_{0.07}Ta_{0.93}Se_2$	1/12.6	domain state
4Hb-$TaSe_2$	1/13	crystal
1T-$NbSe_2$	1/13	crystal
1T-VSe_2	1/16	crystal

Vodeb et al., New J. Phys. (2019) 10.1088/1367-2630/ab3057

Configurational quantum charge liquid

$\psi = |$ 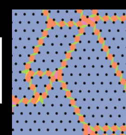 $\rangle + |$ 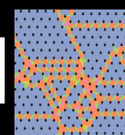 $\rangle + \ldots$

- Domain states are configurationally (nearly) degenerate.[1]
- There is a large configurational entropy
- Which configuration wins is determined by Quantum Darwinism[2] , and interaction with the environment

1. Vodeb et al., *New J. Phys.* (2019)
2. e.g. W. Zurek, *Rev. Mod. Phys.* (2003).
3. Coppersmith et al Phys. Rev. B (1982).

Scanning tunneling microscopy (STM) of some doped and photodoped TMDs

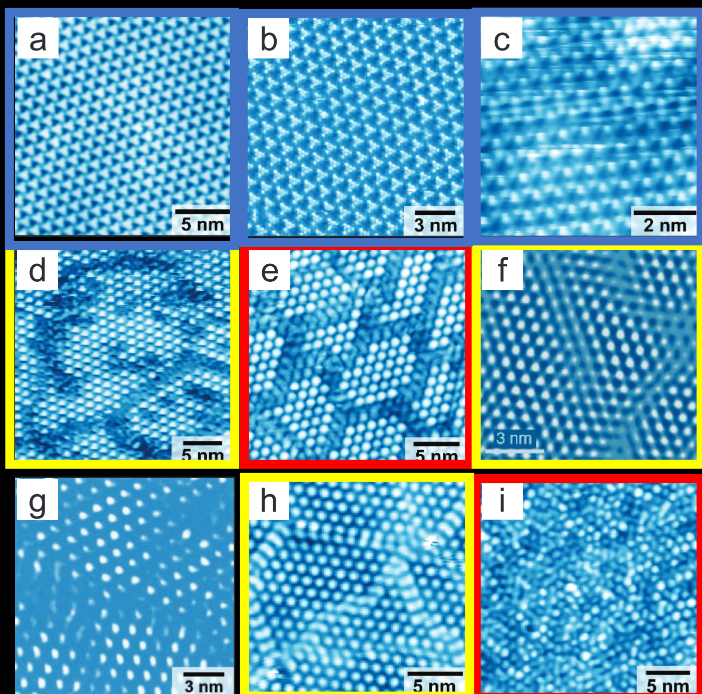

Legend: Superconductors
Superconductors under pressure
Light-induced metastable

Undoped: f_m = integer filling fraction

a) 1T-TaS_2 ($f_m = 1/13$),
b) 1T-$TaSe_2$ ($f_m = 1/13$)
c) 1T-$TiSe_2$ ($f_m = 1/4$).

Doped: f_m in between integer filling fractions

d) 1T-$Ta_{0.99}Fe_{0.01}S_2$ ($f \approx 1/12.6$),
e) photodoped 1T-TaS_2 (fluence $F \simeq 1\ mJ/cm^2$, $f \approx 1/12.6$),
f) 1T-$Cu_{0.08}TiSe_2$ ($f \approx 1/4.2$),
g) 1T-$Ti_{0.07}Ta_{0.93}Se_2$ ($f \approx 1/12.6$)
h) 1T-TaSeS ($f \approx 12.6$).

i) glassy state in photodoped metastable 1T-TaS_2

Vodeb et al., New J. Phys (2019)

Phase diagram of Wigner crystals in Transiti

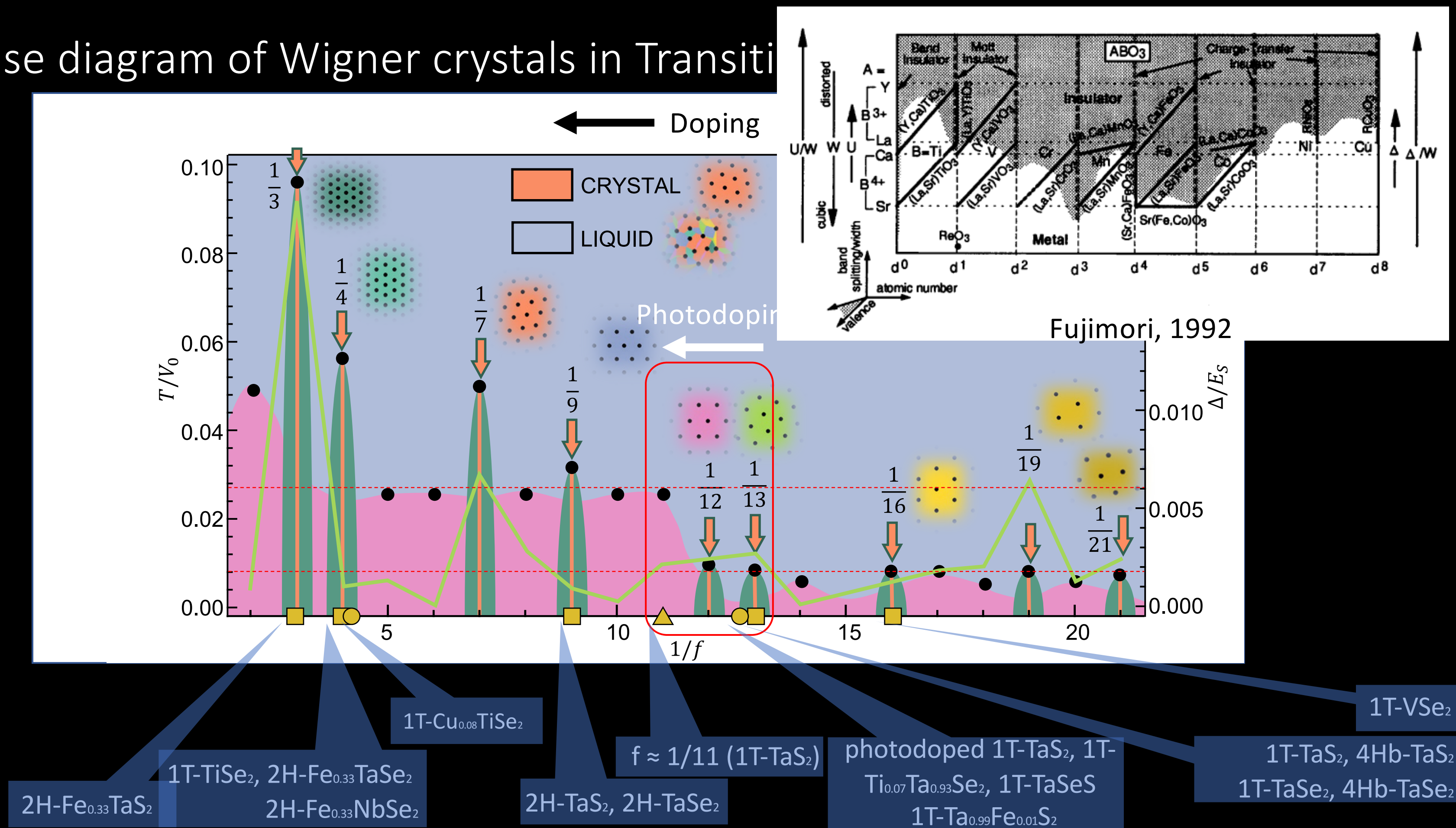

Vodeb et al, *New J. Phys.*, (2019)

A time-domain phase diagram in 1T-TaS_2

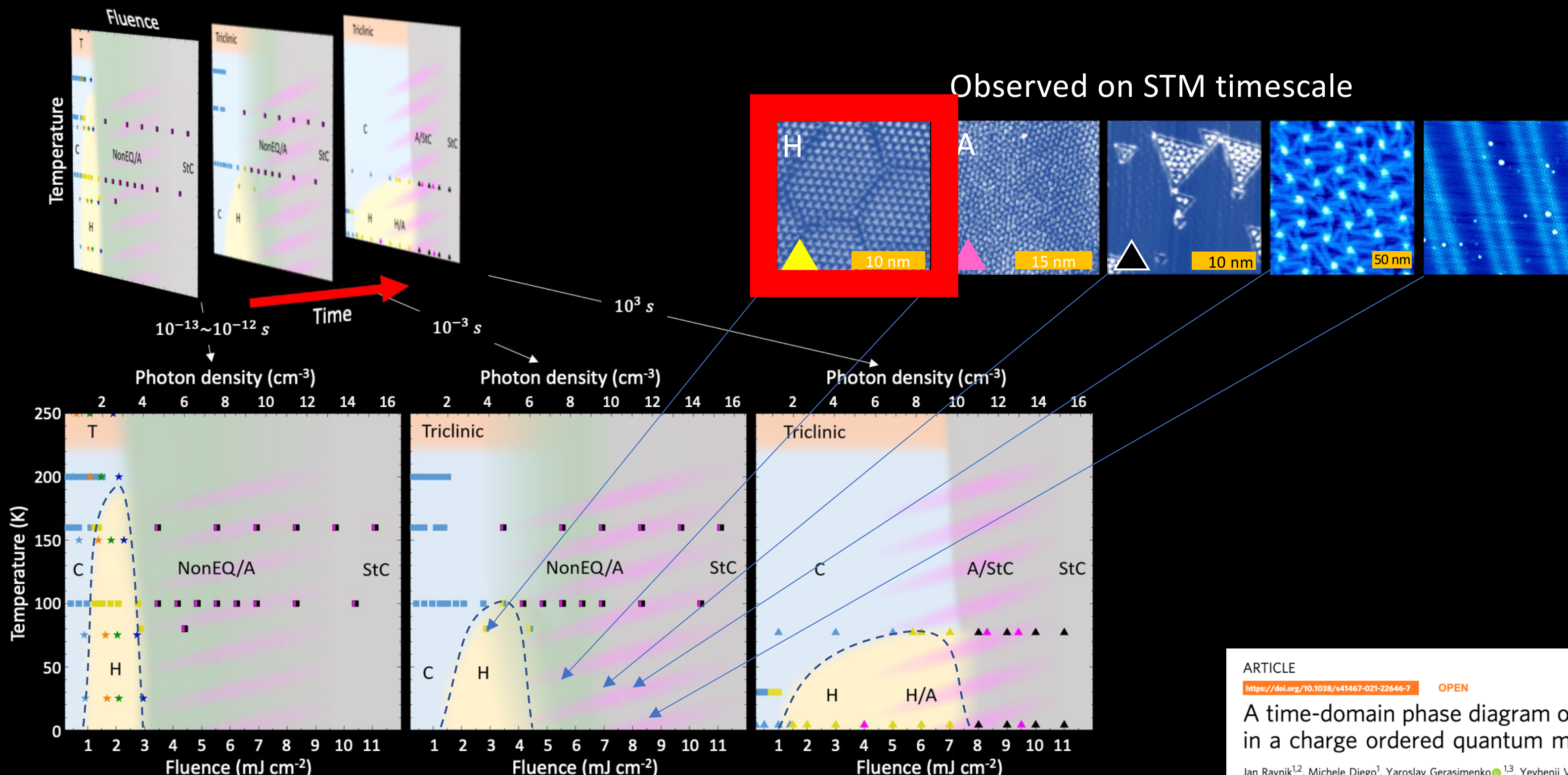

ARTICLE

https://doi.org/10.1038/s41467-021-22646-7 OPEN

A time-domain phase diagram of metastable states in a charge ordered quantum material

Jan Ravnik[1,2], Michele Diego[1], Yaroslav Gerasimenko[1,3], Yevhenii Vaskivskyi[1], Igor Vaskivskyi[1,3], Tomaz Mertelj[1,3], Jaka Vodeb[1] & Dragan Mihailovic[1,3,4]

NATURE COMMUNICATIONS | (2021)12:2323 |

The photoinduced hidden state: chiral domain order

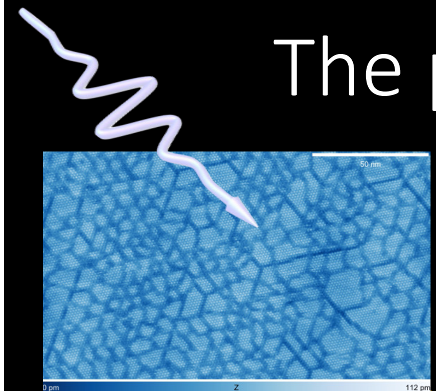

Displacement vector $\vec{D}$ between adjacent domains

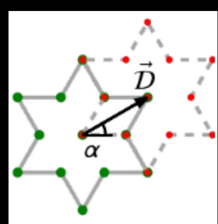

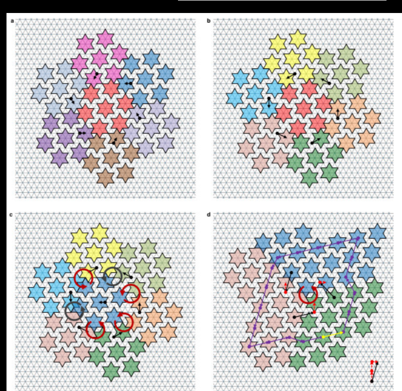

Experimental STM data

Displacement distance $|\vec{D}|$

Displacement angle $\boldsymbol{\alpha}$

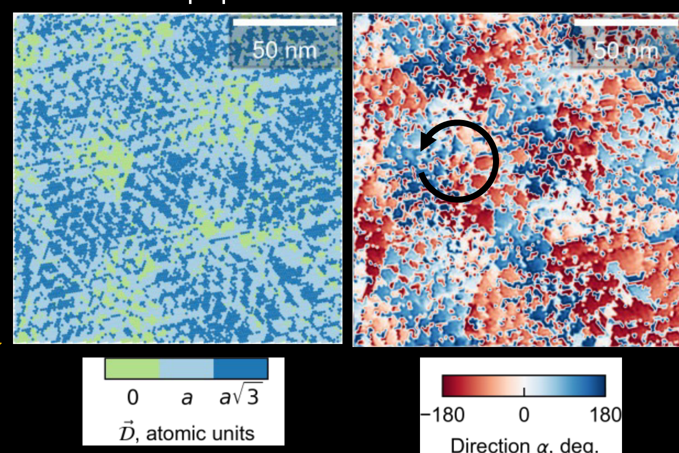

Simulation of $\boldsymbol{\alpha}$

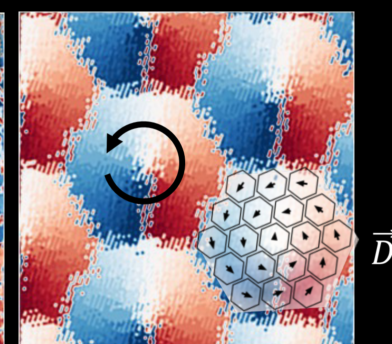

Gerasimenko et al., npj Quantum Materials, **4,** 32 (2019)

Topologically non-trivial vertices in the ’hidden’ state

Color code:

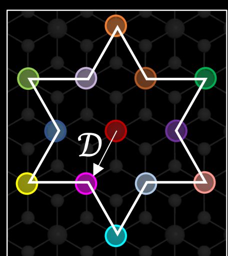

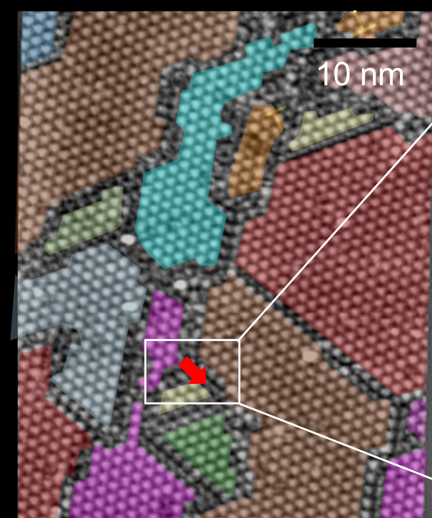

Burgers’ vector constructions

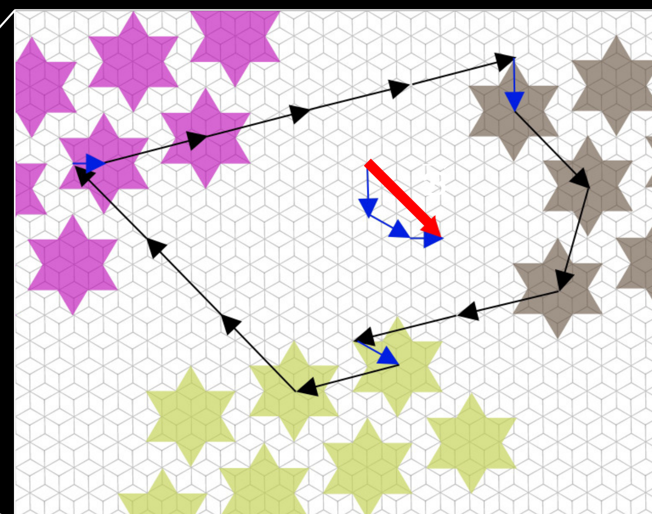

The H state has topologically protected defects where $\overrightarrow{B} \neq 0$

Gerasimenko et al., npj Quantum Materials, **4,** 32 (2019)

Vertices as dislocations

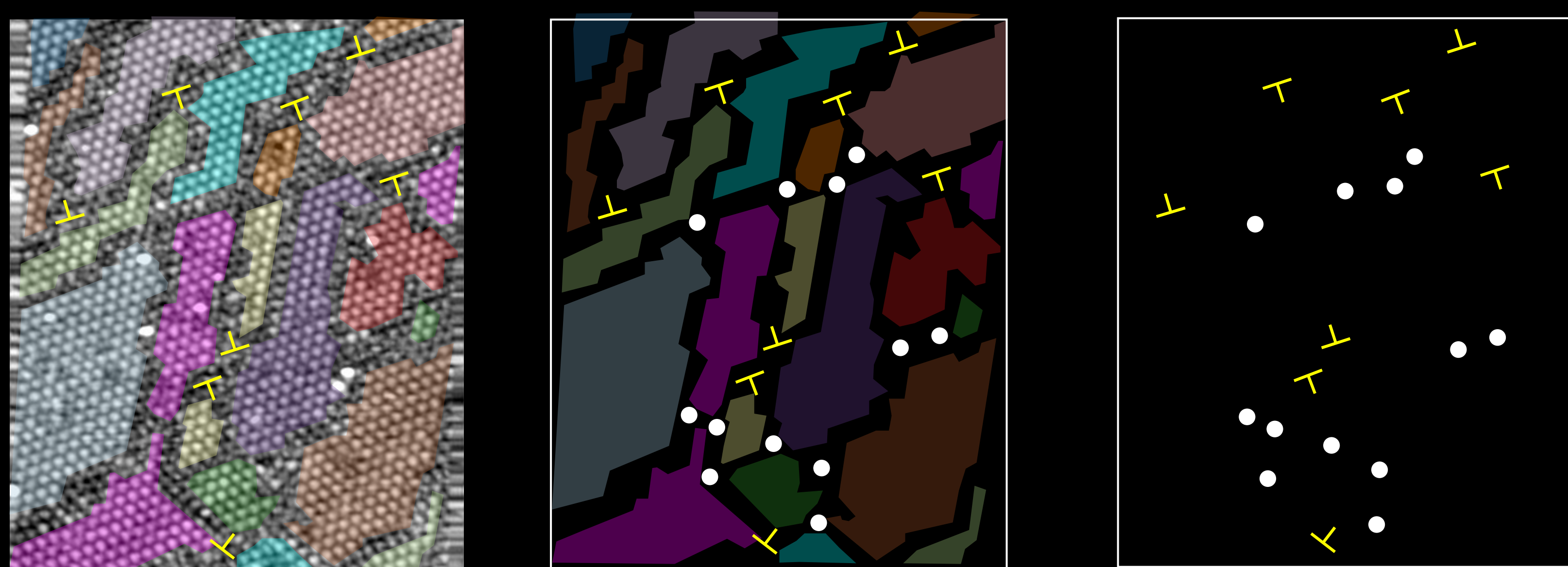

Wigner-Seitz cell constructions of the CDW superlattice: Charge is associated with $B \neq 0$ defects

STM image of H state

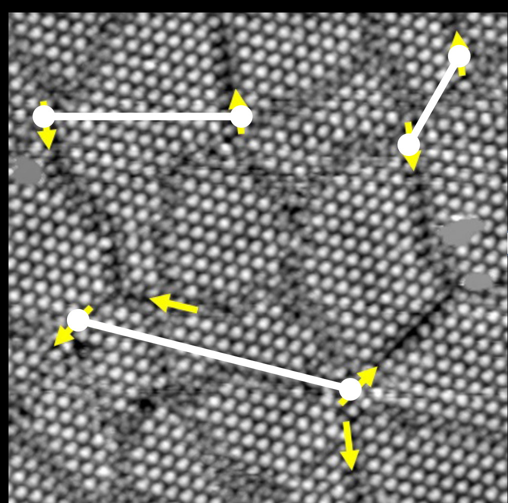

Burgers vectors

Wigner-Seitz construction of H state

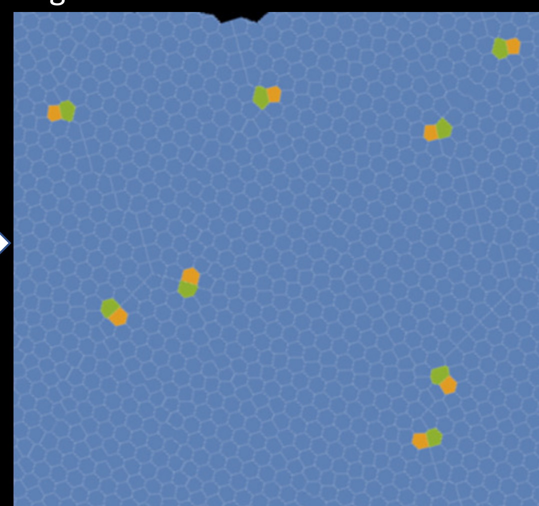

Disclinations | Dislocations

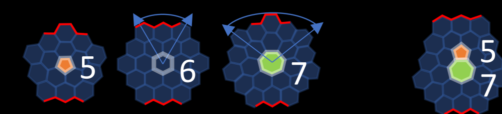

Add 1 electron:

3 x 6 → 2 x 7 +2 x 5

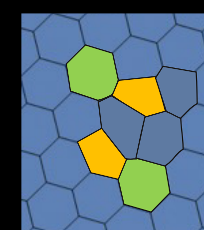

Add 1 hole:

5 x 6 -> 2 x 7 +2 x 5

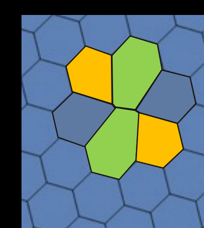

CLG Monte Carlo simulation and experiment
(Wigner-Seitz constructions)

MC calculation of a polaronic Wigner crystal (CLG)

Single particle doping

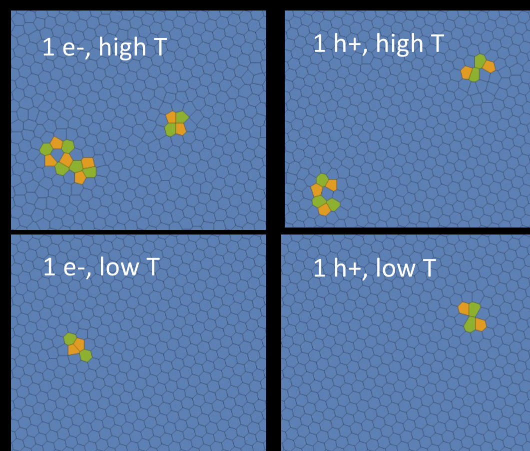

Multiple particle doping

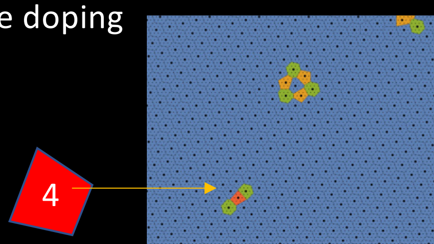

STM of H state (4K)

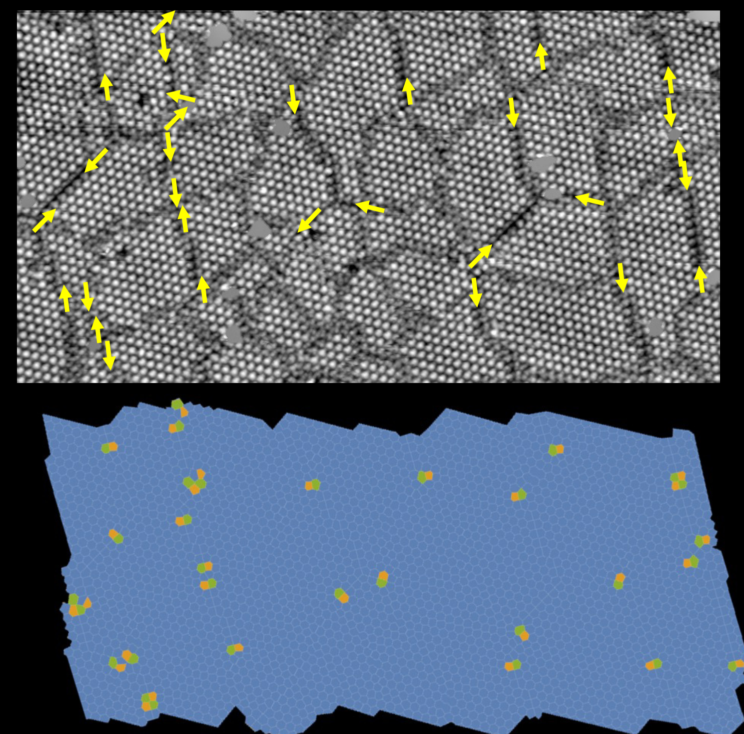

Experiments show that the electrons are topologically entangled objects.

CLG Monte Carlo simulation and experiment

(Wigner-Seitz constructions)

MC calculation of a polaronic Wigner crystal (CLG)

Single particle doping

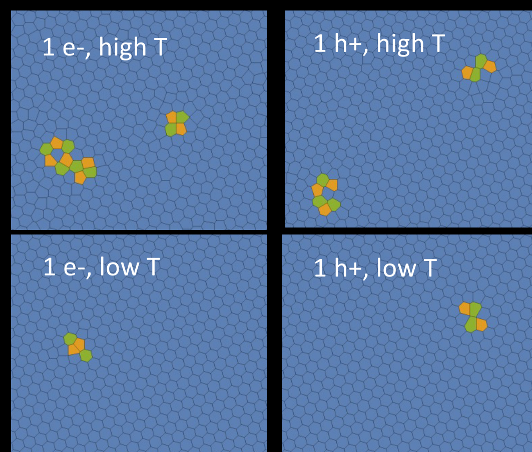

Multiple particle doping

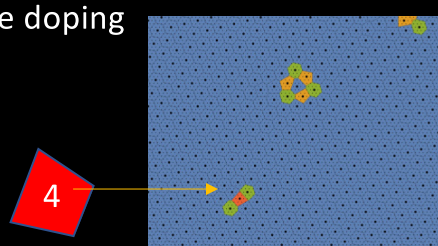

STM of H state (4K)

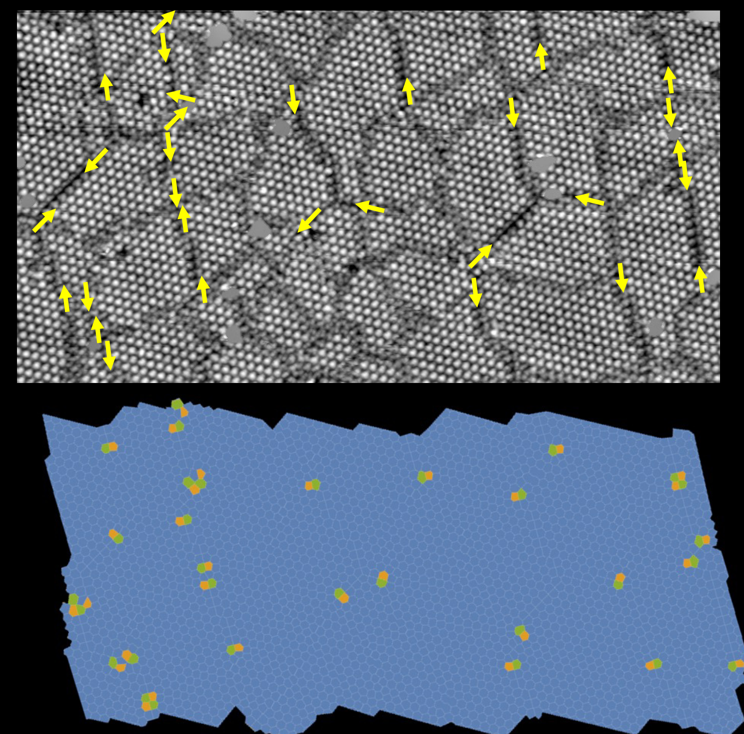

Experiments show that the electrons are topologically entangled objects.

Defect dynamics: spontaneous relaxation through configurational states

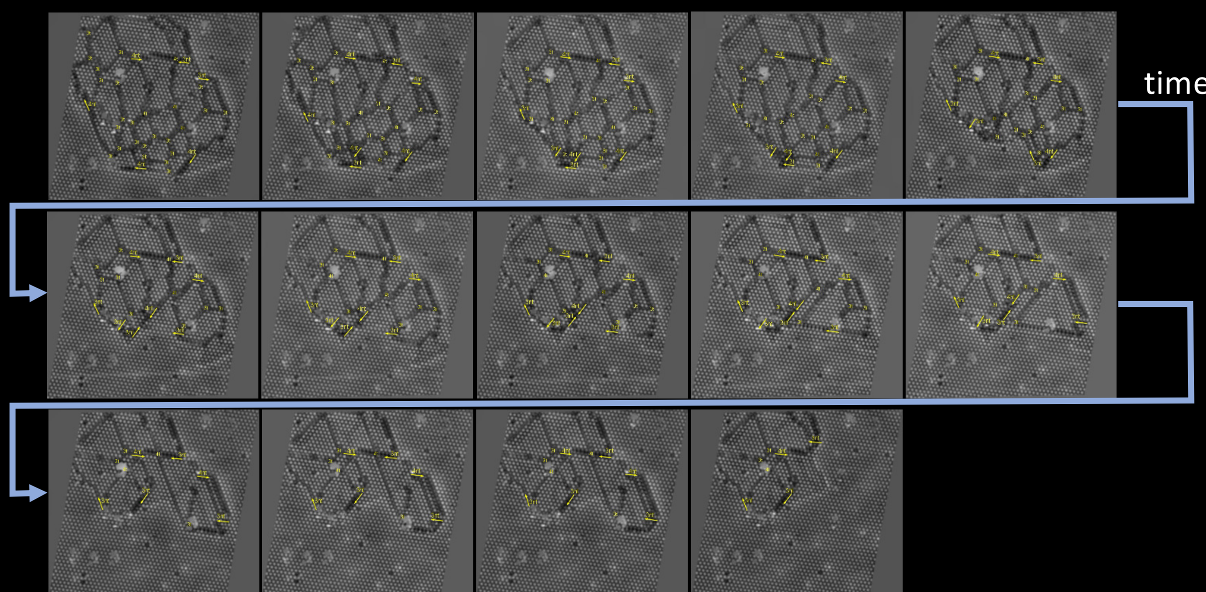

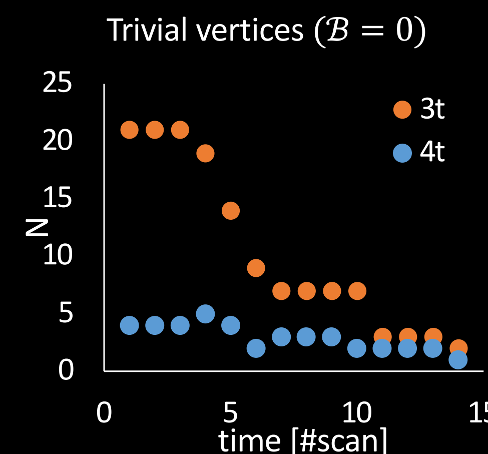

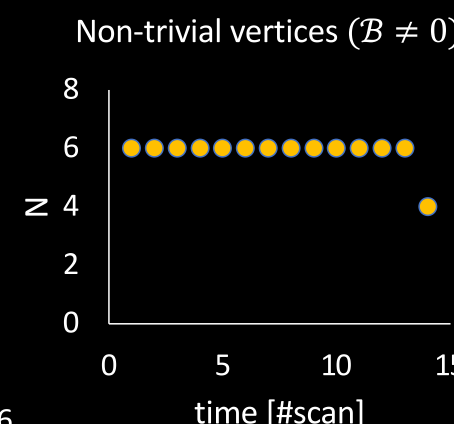

Conclusion: Topologically non-trivial defects stabilize the ‘hidden’ domain state

Kranjec et al, *Symmetry* 2022, 14, 926. https:// doi.org/10.3390/sym14050926

Defect dynamics under applied electric field

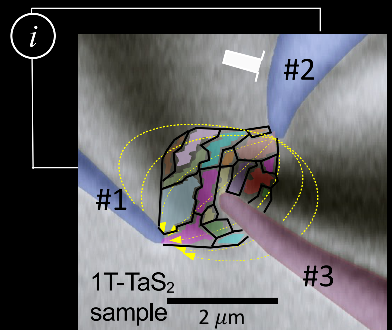

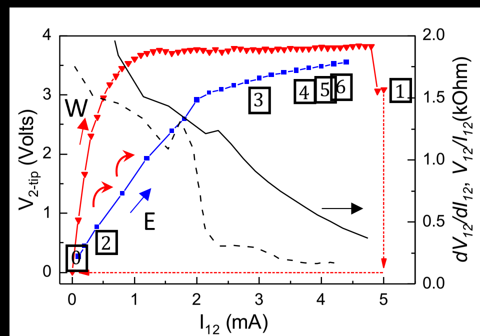

Displacement vectors: colour code

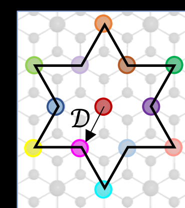

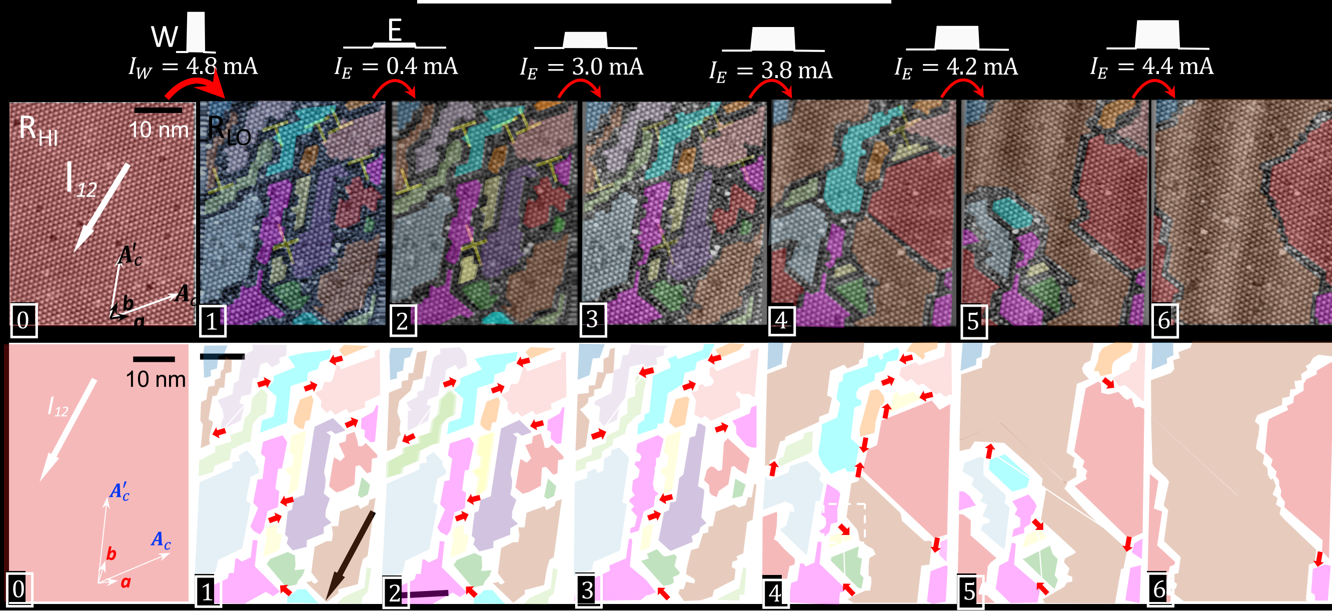

Non-trivial defect annihilation

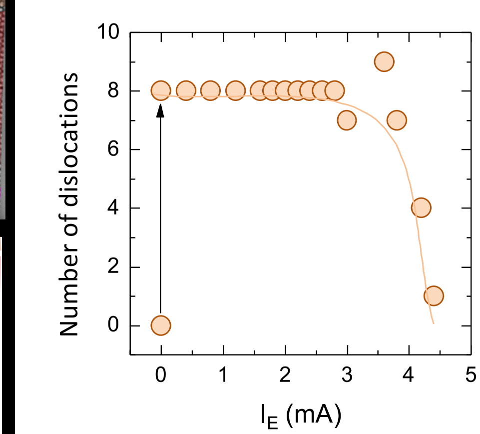

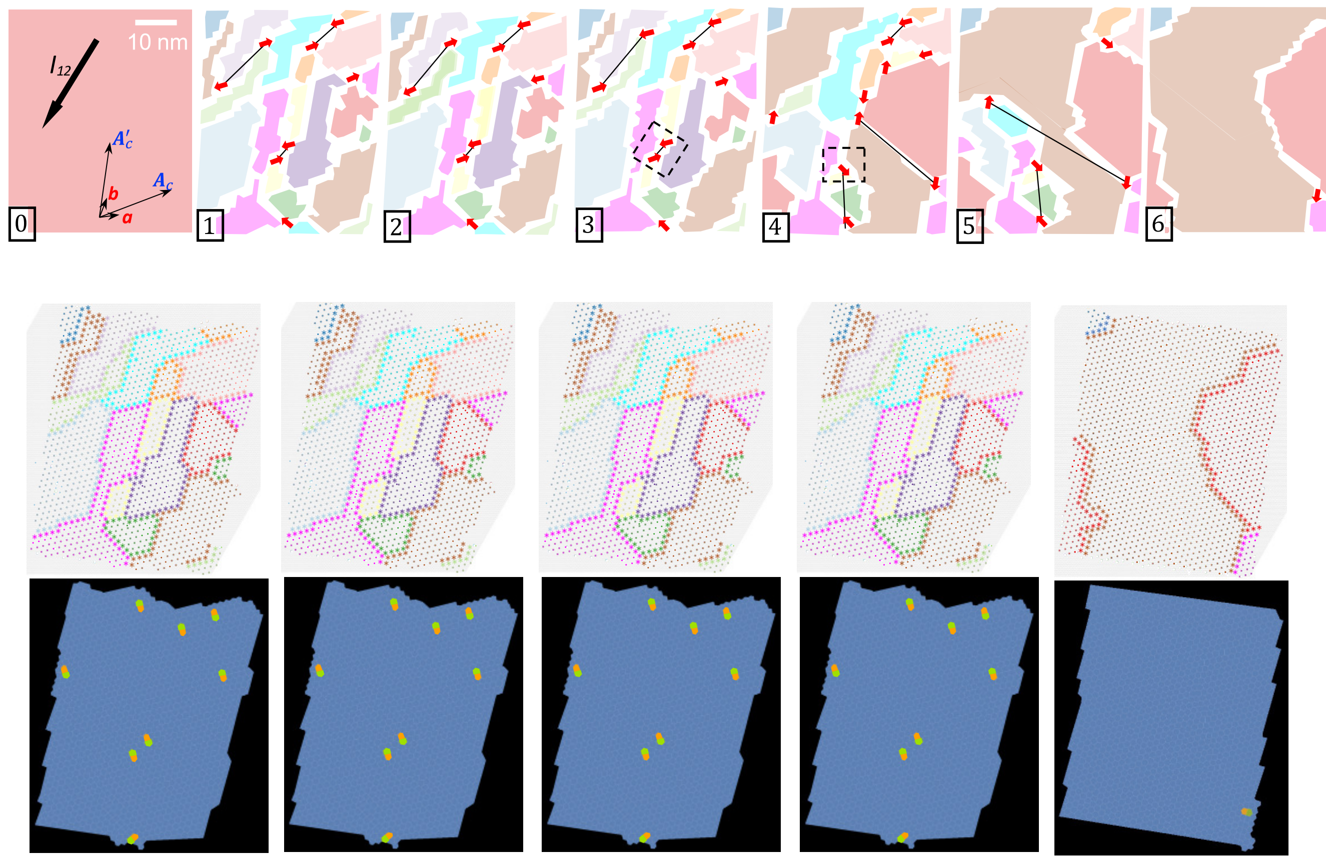

Mraz, Kranjec, Karpov

Interlayer ordering

Occasionally, the CDWs are stacked without a phase shift

The vertices are usually in the centre of domains in the next layer

From experiment

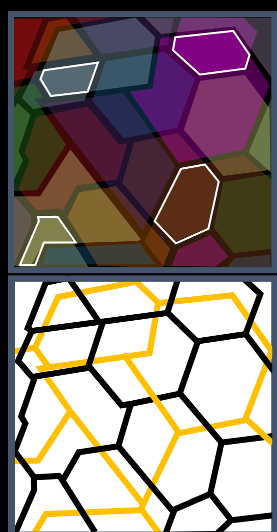

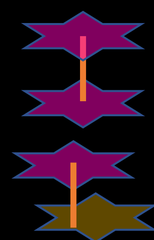

Band structure calculations

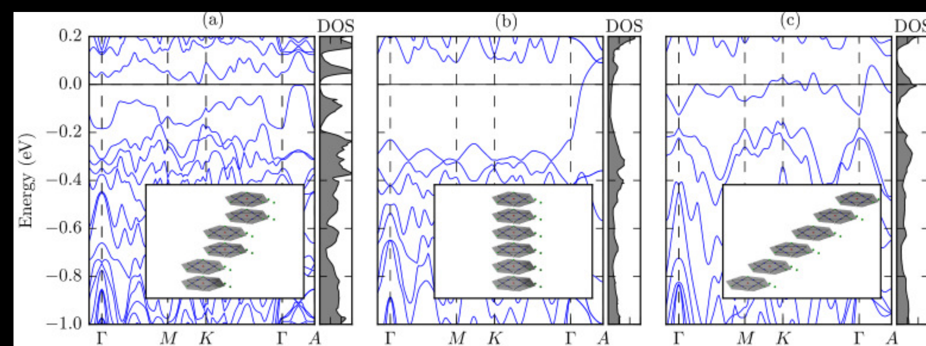

1. Butler, C. J., Yoshida, M., Hanaguri, T. & Iwasa, Y. Mottness versus unit-cell doubling as the driver of the insulating state in 1T-TaS2. *Nat Commun* **11**, 2477 (2020).
2. Stahl, Q. *et al.* Collapse of layer dimerization in the photo-induced hidden state of 1T-TaS2. *Nat Commun* **11**, 1–7 (2020).
3. Ritschel, T., Berger, H. & Geck, J. Stacking-driven gap formation in layered 1T-TaS2. *Phys Rev B* **98**, 1–8 (2018).

Quantum tunneling between configurational states

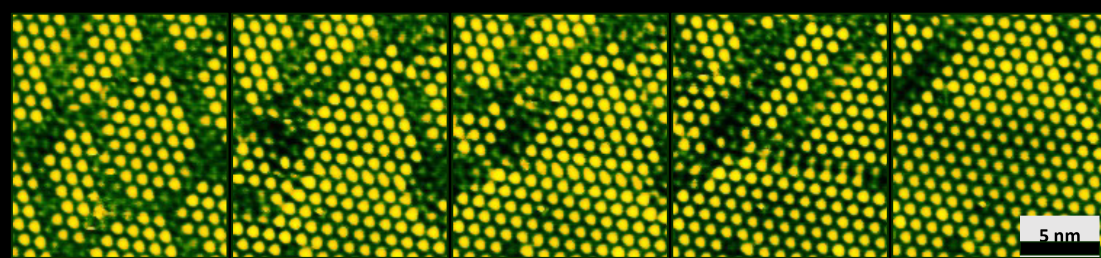

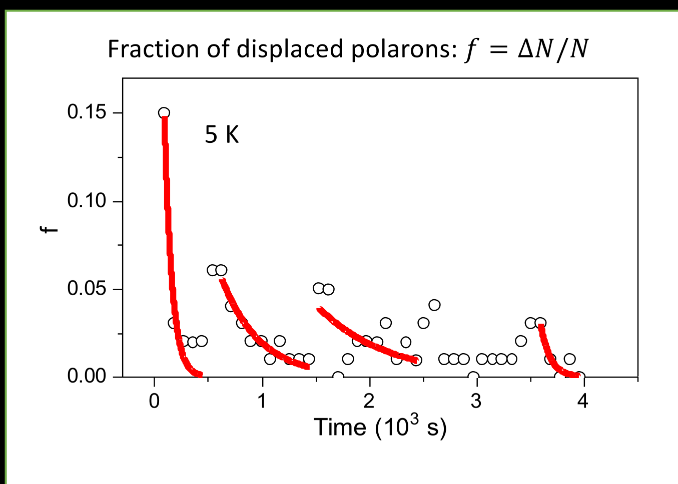

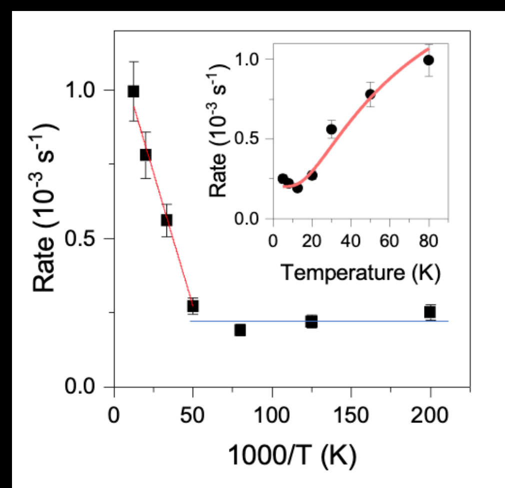

Total relaxation rate (fit):

$$R(T) = R_q + R_0 \exp\left(-\frac{E_B}{k_B T}\right),$$

Quantum tunneling Activated hopping

WKB estimate of the tunneling rate

$$R_q = \nu \exp\left(-2w\sqrt{2m^* E_b/\hbar^2}\right)$$

For a 1000 electron domain,

$$R_q = 2.2 \pm 0.3 \times 10^{-4} s^{-1}$$ (reasonable)

Tip-enhanced relaxation?

Relaxation with tip scanning

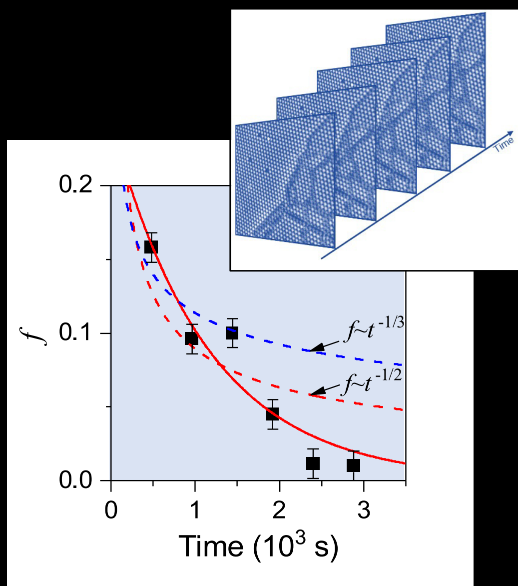

Relaxation with NO tip scanning

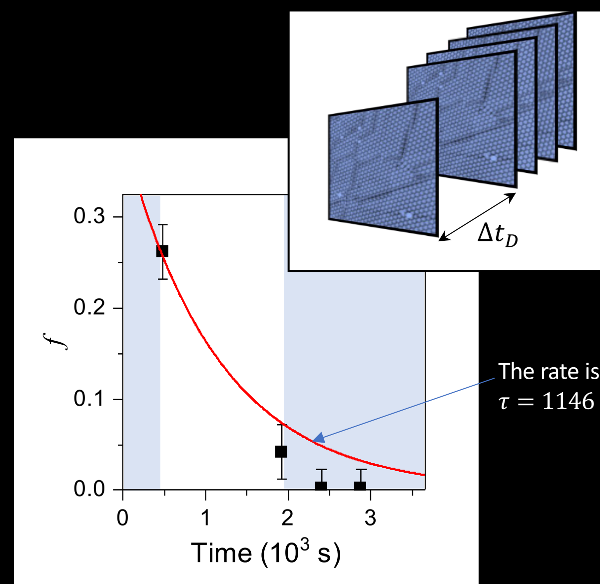

The rate is similar: a fit gives $\tau = 1146 \pm 38\,s$ (for both)

Schroedinger's cat measurements

D-wave annealing (direct embedding)

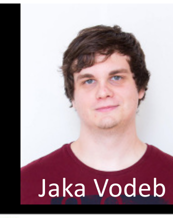

Quantum annealing using the transverse field Ising model:

$$H = -\frac{A(s)}{2}\left(\sum_i \sigma_i^x\right) + \frac{B(s)}{2}\left(\sum_i h_i\sigma_i^z + \sum_{i>j} J_{i,j}\sigma_i^z\sigma_j^z\right)$$

Annealing protocol:

$$H = -AH_x + BH_z$$
$$Z = Tr(\exp(-\beta H))$$
$$\beta H = \beta A\left(-H_x + \frac{B}{A}H_z\right)$$
$$\frac{A}{k_B T} = \frac{1}{T_{eff}} \qquad T_{eff} = \frac{k_B T}{A}$$

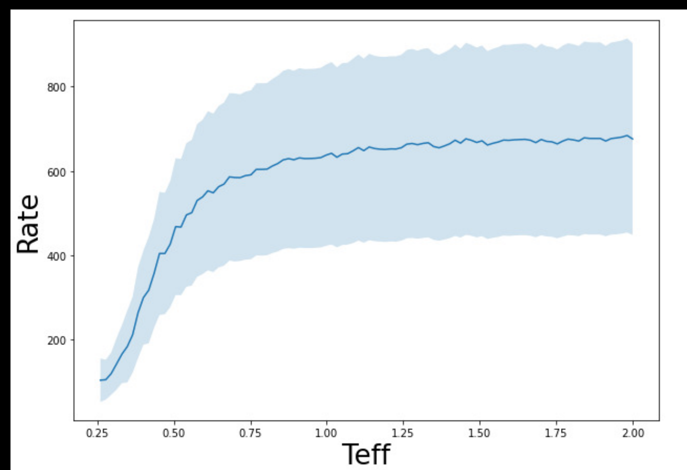

Temperature scale:

$$T = 16\, mK$$
$$k_B T = 1.38 \pm 0.01\, \mu eV$$

J. Vodeb et al., unpub. (2022)

$Inital\ state: all\ 1$

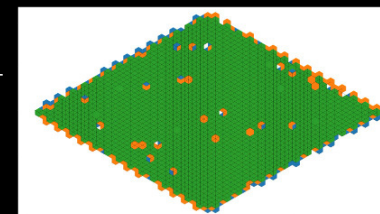

T_{low}

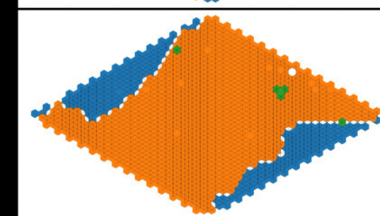

T_{med}

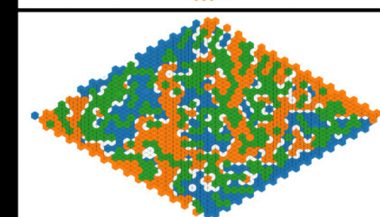

T_{high}

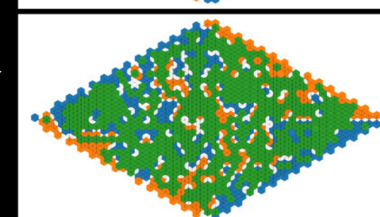

A time-domain phase diagram in 1T-TaS_2

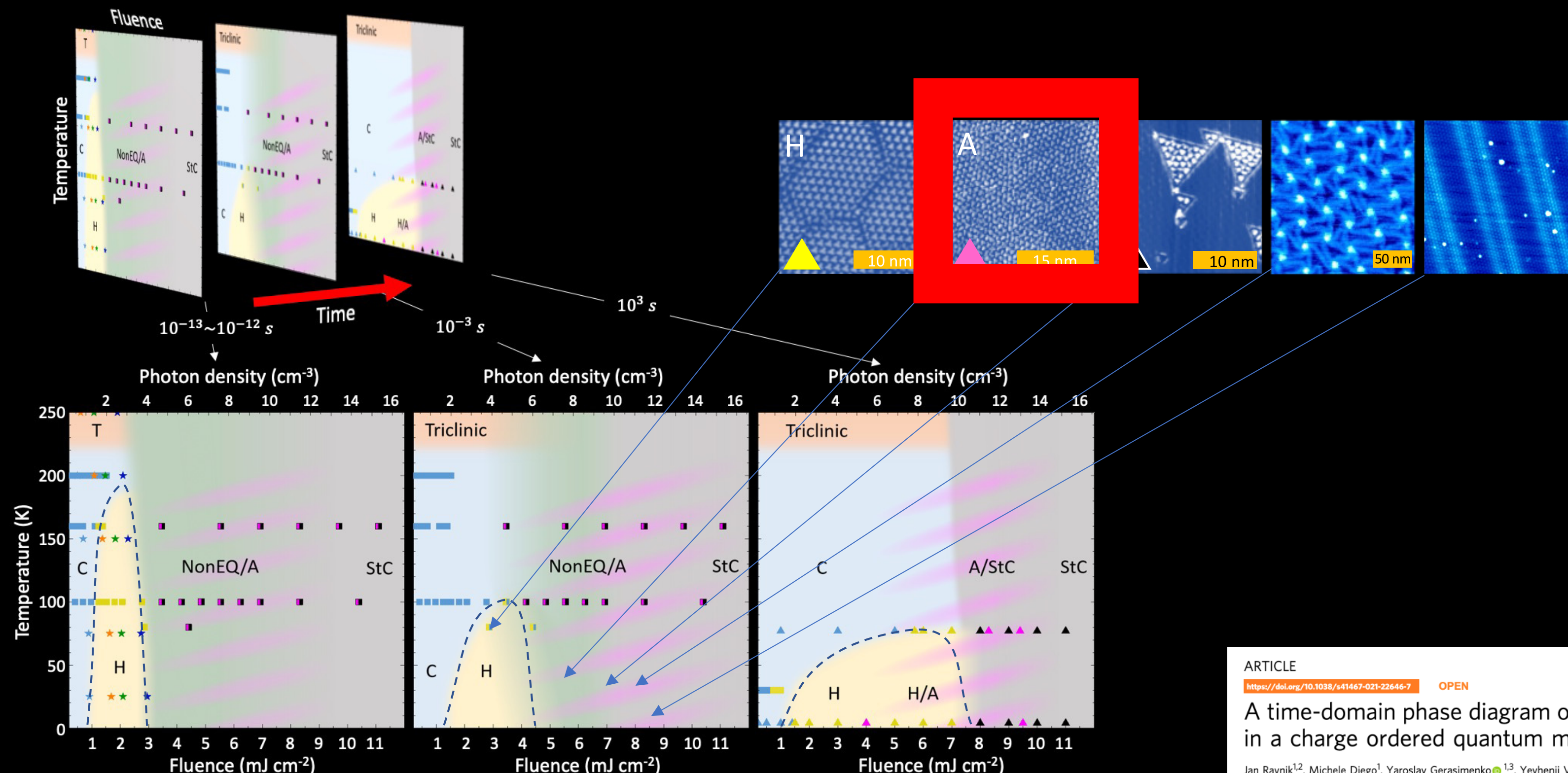

ARTICLE

https://doi.org/10.1038/s41467-021-22646-7 OPEN

A time-domain phase diagram of metastable states in a charge ordered quantum material

Jan Ravnik[1,2], Michele Diego[1], Yaroslav Gerasimenko[1,3], Yevhenii Vaskivskyi[1], Igor Vaskivskyi[1,3], Tomaz Mertelj[1,3], Jaka Vodeb[1] & Dragan Mihailovic[1,3,4]

NATURE COMMUNICATIONS | (2021)12:2323 |

Jamming transition to an amorphous Wigner glass

$2.5 \sim 3\ mJ/cm^2$

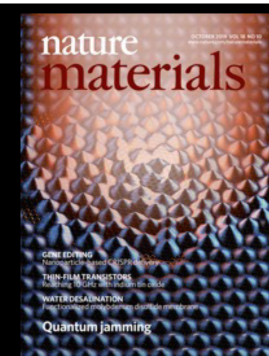

Gerasimenko, et al.
Nature Materials (2019)

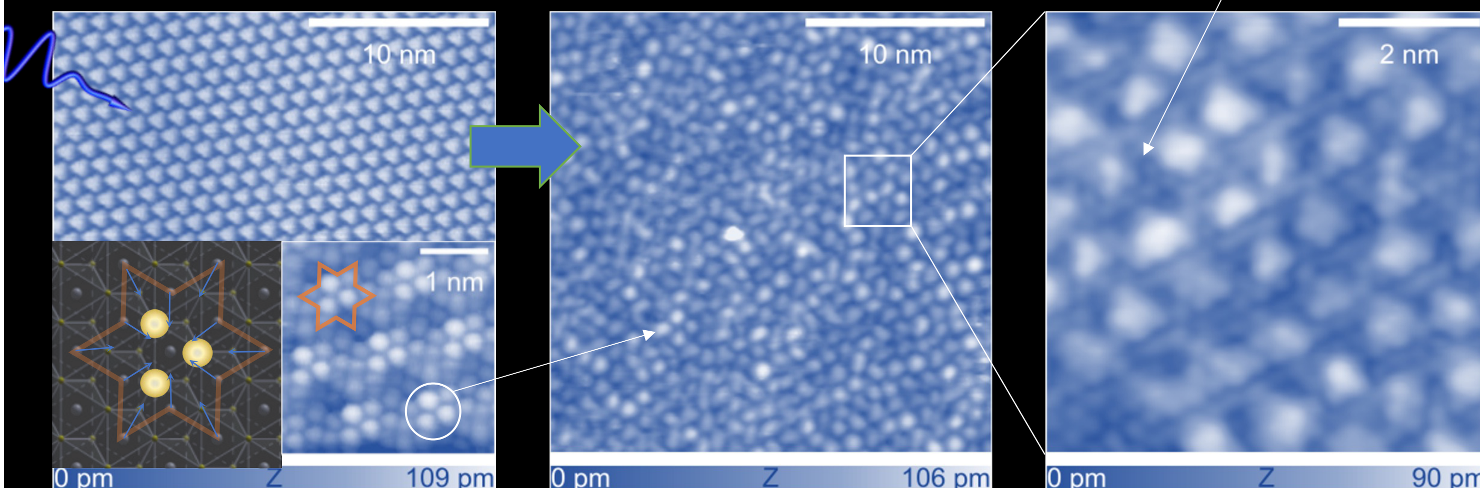

Localized electron density (nm^{-2})

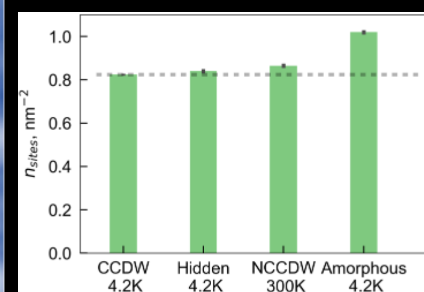

Hyperuniformity and jamming transitions

Classical jamming

Pebbles

Kayak jam

Plant cells

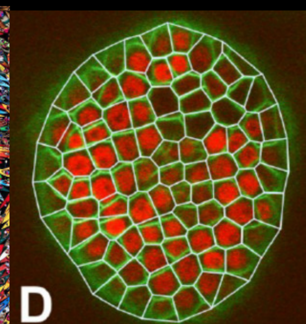

Traffic jams

Neutron stars?

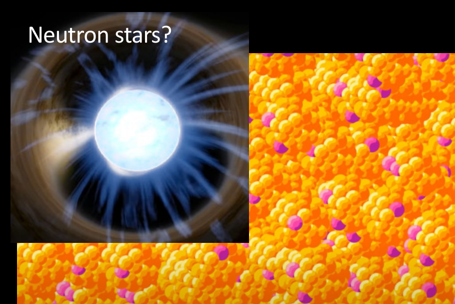

Number variance in simple **random** systems:

$\sigma_N^2(R) \sim R^d$, where d=dimensionality

Number variance in **hyperuniform** systems, for $R \to \infty$:

$$\sigma_N^2(R) \sim \begin{cases} R^{d-1}, & \alpha > 1, \\ R^{d-1}\ln R, & \alpha = 1, \\ R^{d-\alpha}, & 0 < \alpha < 1. \end{cases} \qquad (R \to \infty).$$

<u>Structure factor in hyperuniform systems :</u>

Definition of α : $\lim_{|k|\to 0} S(\boldsymbol{k}) = 0$

$$S(k) \sim |k|^{\alpha}$$

Torquato, S. Hyperuniformity and its generalizations. *Physical Review E* **94**, 022122 (2016).

CLG model prediction of the N-gon statistics in the amorphous (A) phase

Experiment (STM, 4K, 2 mJ/cm²)

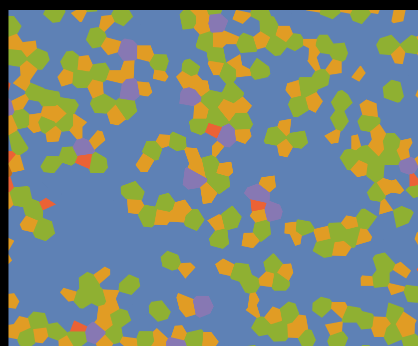

CLG model calculation (MC simulation)

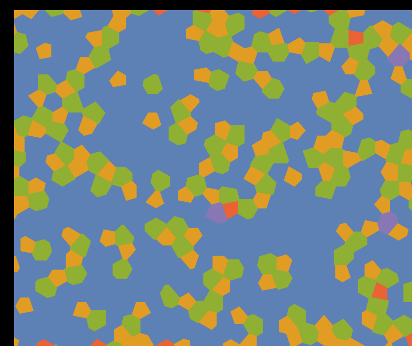

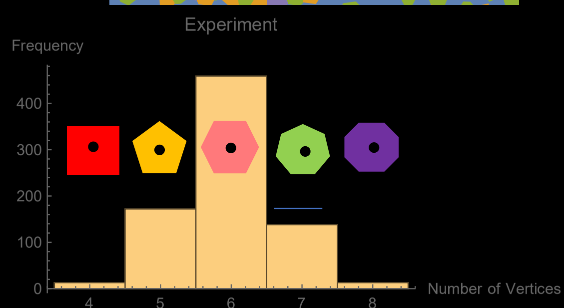

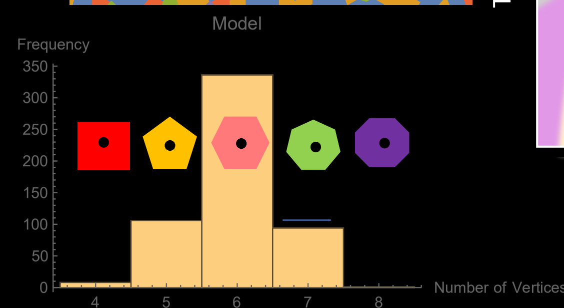

MC Simulations

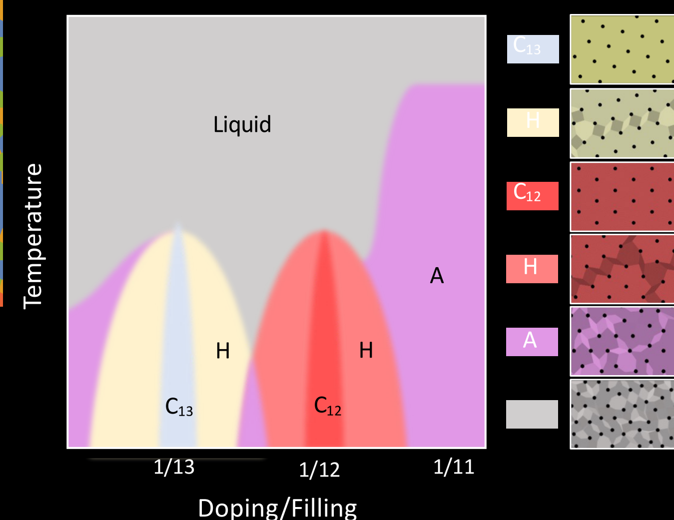

Jaka Vodeb, unpub. work

Can the *quantum* dynamics be described in terms of fractons?

PHYSICAL REVIEW LETTERS **120,** 195301 (2018)

Editors' Suggestion | Featured in Physics

Fracton-Elasticity Duality

Michael Pretko and Leo Radzihovsky
Department of Physics and Center for Theory of Quantum Matter, University of Colorado, Boulder, Colorado 80309, USA

PHYSICAL REVIEW B **92**, 235136 (2015)

A new kind of topological quantum order: A dimensional hierarchy of quasiparticles built from stationary excitations

Sagar Vijay, Jeongwan Haah, and Liang Fu

"The conservation laws of fracton gauge theories provide a convenient and systematic tool for encoding and analyzing the dynamics of crystal defects."

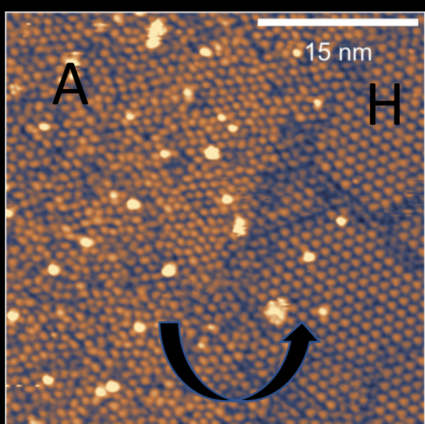

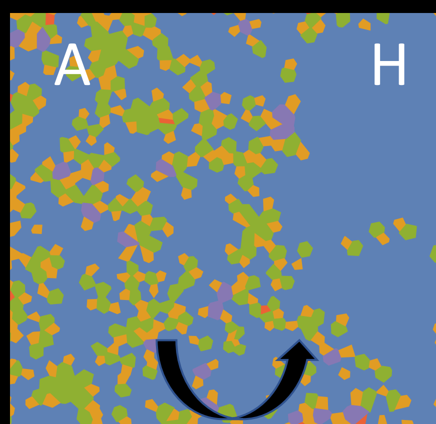

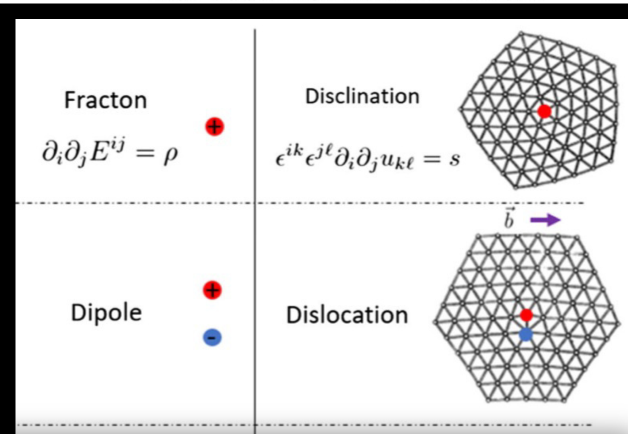

immobile

Mobile (glide)

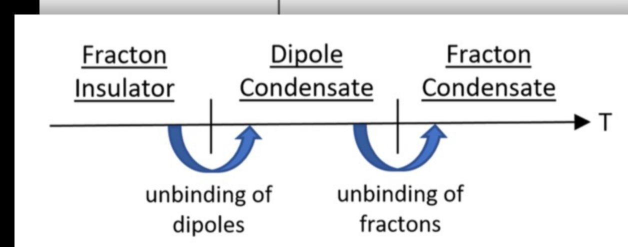

A time-domain phase diagram in $1T\text{-}TaS_2$

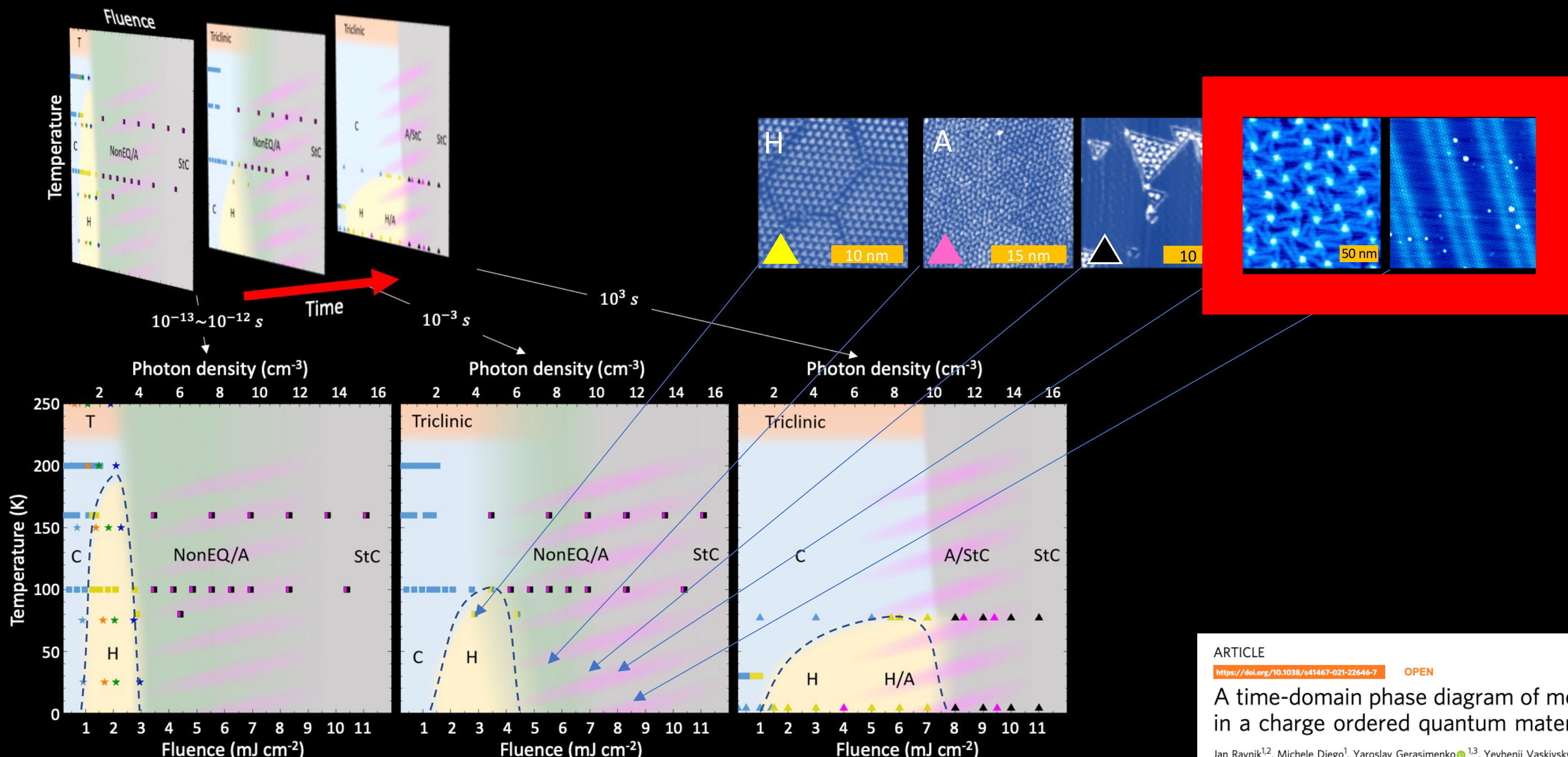

ARTICLE

https://doi.org/10.1038/s41467-021-22646-7

OPEN

A time-domain phase diagram of metastable states in a charge ordered quantum material

Jan Ravnik[1,2], Michele Diego[1], Yaroslav Gerasimenko[1,3], Yevhenii Vaskivskyi[1], Igor Vaskivskyi[1,3], Tomaz Mertelj[1,3], Jaka Vodeb[1] & Dragan Mihailovic[1,3,4]

NATURE COMMUNICATIONS | (2021)12:2323 |

Light-induced single-layer polytype transformation – topological CDWs

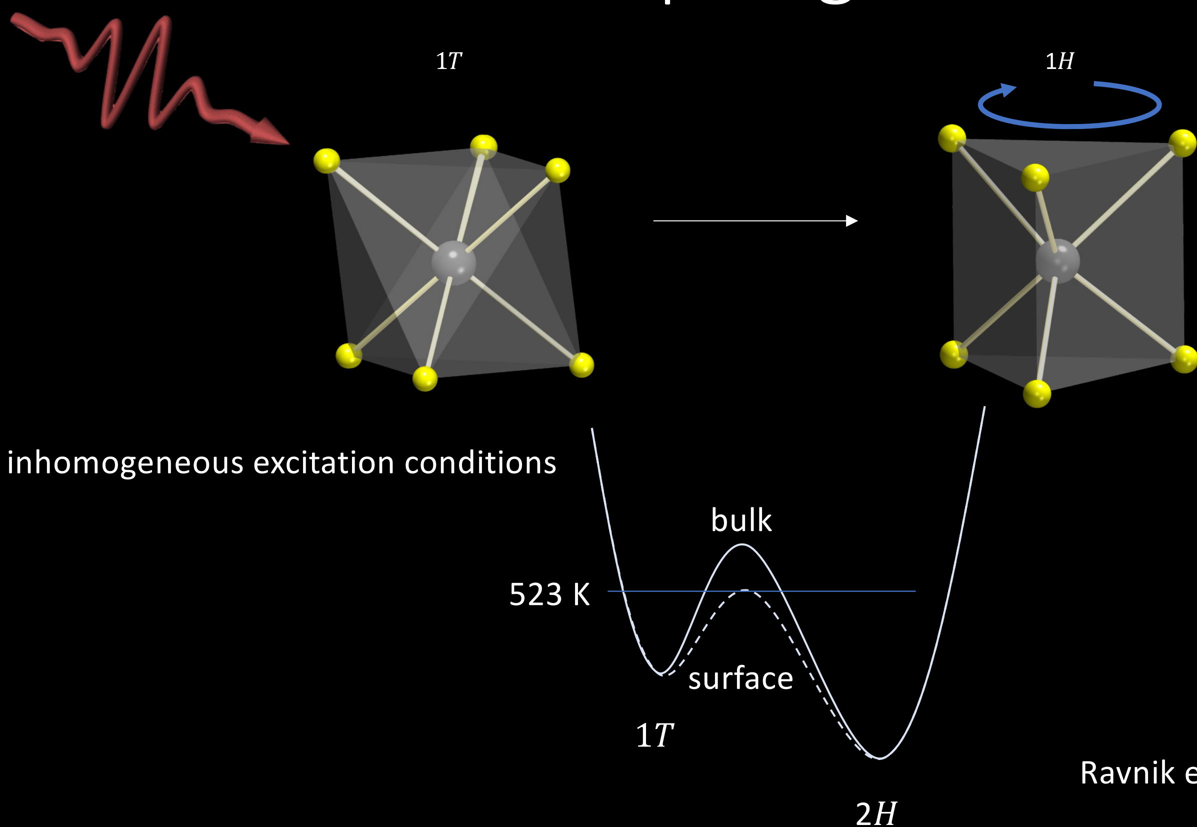

Control: inhomogeneous excitation conditions

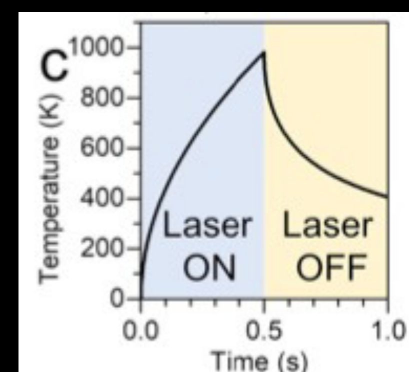

Ravnik et al., ACS *Nano materials* (2019)

Light-induced 1H-1T heterostructure of TaS_2

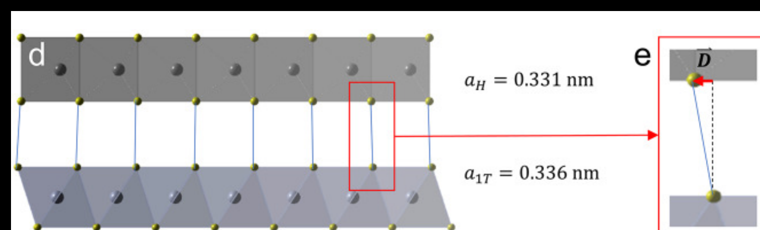

$\vec{D} - displacement\ vector\ field$

We may expect the charge density wave to adapt to the Moiré pattern (or discommensurations)

Ravnik et al., ACS *Nano materials* (2019)

Topological charge density wave patterns of a 1H/1T-TaS_2 bilayer

Stripe phase

Trigonal lattice

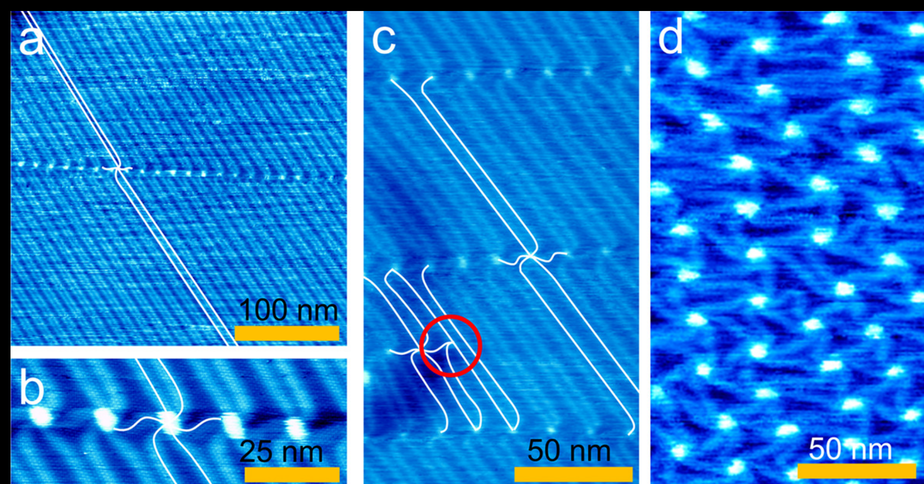

Ravnik et al., ACS *Applied Nano materials 2, 3743* (2019)

Topology of the Moiré electron density map of a 1H/1T-TaS_2 bilayer.

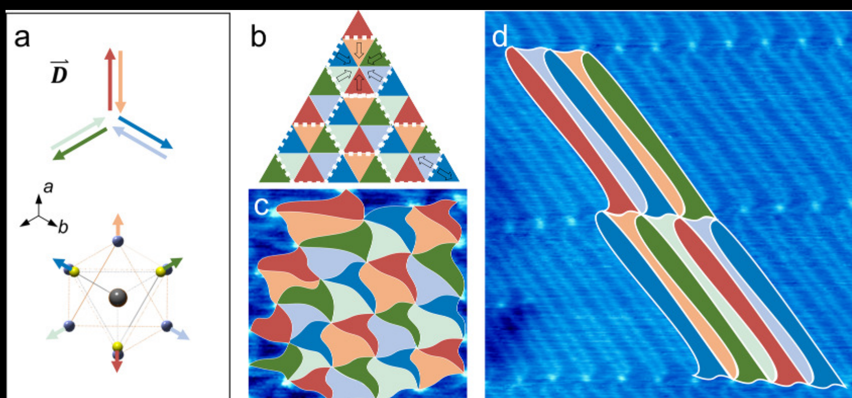

The topology of the CDW is described by the cyclic group Z_k:

$$Z_6 = Z_3 \times Z_2$$

Z_n = 2 the number of possible antiphase domains (colour map)
----- Antiphase domain boundaries
Z_m = 3 the number m of directional variants of $\vec{D}$ (arrows)

Ravnik et al., ACS *Applied Nano materials 2, 3743* (2019)

Topology: a triangular density wave network

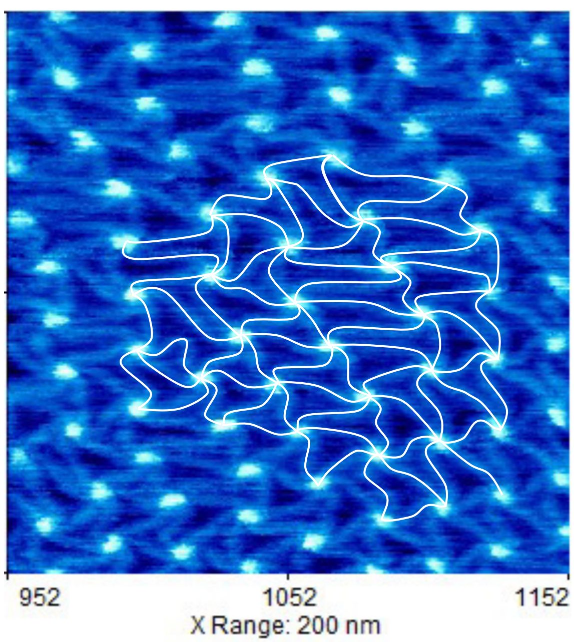

No visible symmetry

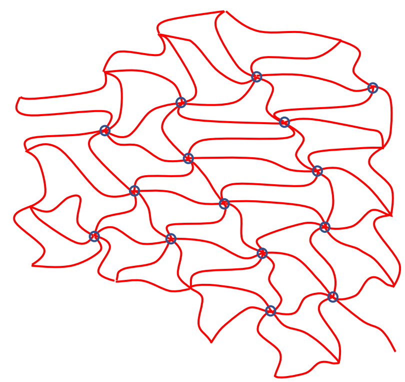

T_n grid graph

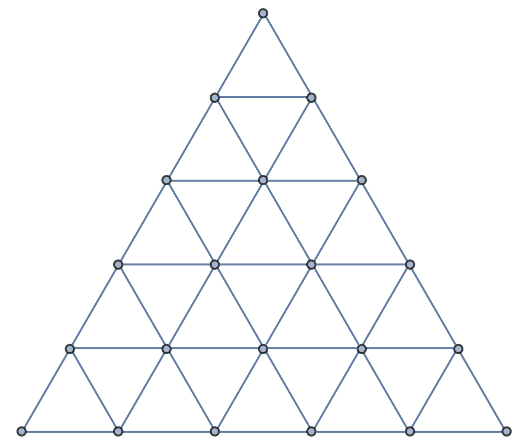

Topological defects: dislocations in electron density maps of a 1H/1T-TaS_2 bilayer.

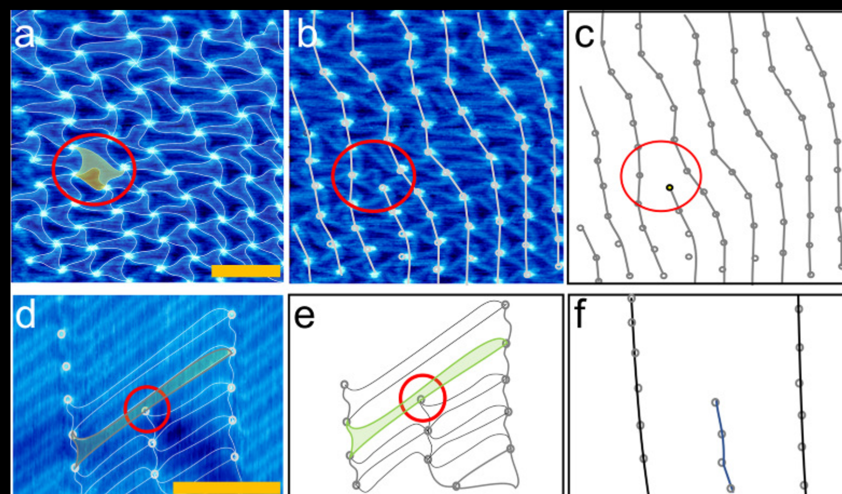

Dislocations in the electronic density wave pattern

Ravnik et al., ACS *Applied Nano materials 2, 3743* (2019)

Phase diagram of a discommensurate 2D honeycomb network

Surface Science 97 (1980) 219–242
© North-Holland Publishing Company

COMMENSURATE–INCOMMENSURATE TRANSITION OF KRYPTON MONOLAYERS ON GRAPHITE: A LOW TEMPERATURE THEORY

Jacques VILLAIN

Département de Recherche Fondamentale, Laboratoire de Diffraction Neutronique, Centre d'Etudes Nucléaires de Grenoble, 85 X, F-38041 Grenoble Cédex, France

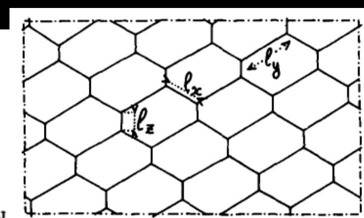

Free energy of a discommensured 2D honeycomb network:

$$F = 2\Lambda\nu + \mu L - T \log G(g, L)$$

vertices, segment length, entropy

This approximation can only be used for positive values of μ. For negative μ indeed, the minimum of F is $-\infty$ for $l_x = \infty$ and $l_y = l_z = 0$. This result is complete nonsense. Thus, the model can only be used near the C–I transition, and for positive Λ.

Experiment:

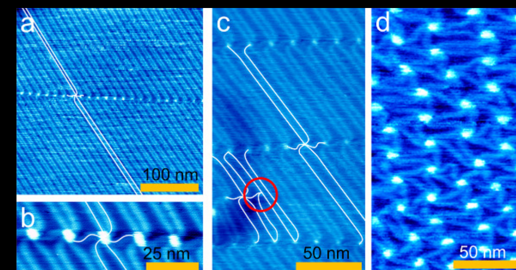

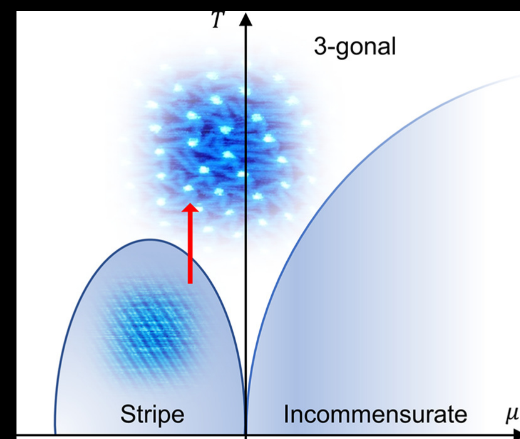

Villain 1982, Ravnik et al., ACS *Applied Nano materials 2, 3743* (2019)

A time-domain phase diagram in 1T-TaS_2

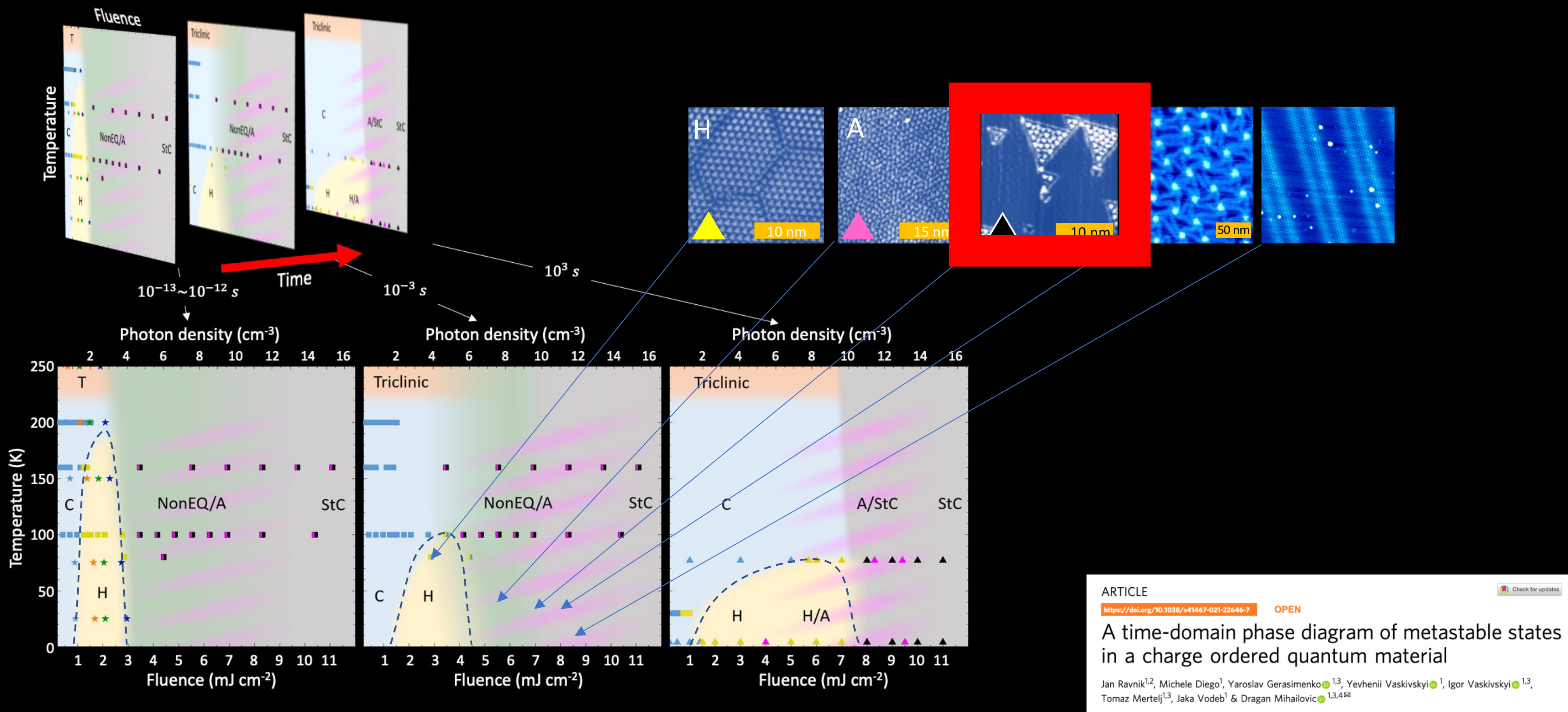

NATURE COMMUNICATIONS | (2021)12:2323 |

Laser-induced

1T-1H polytype phase separation

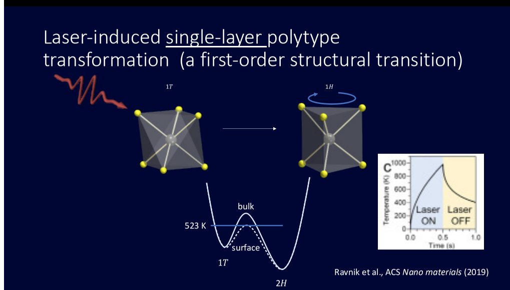

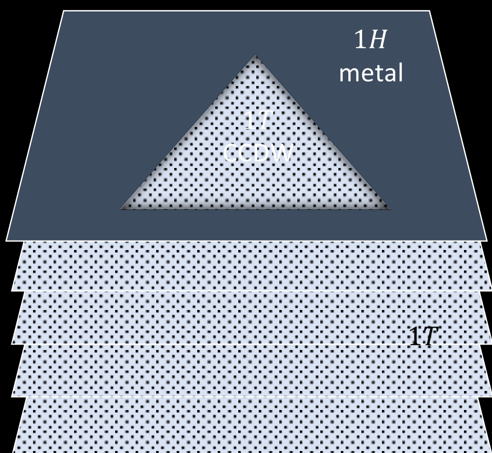

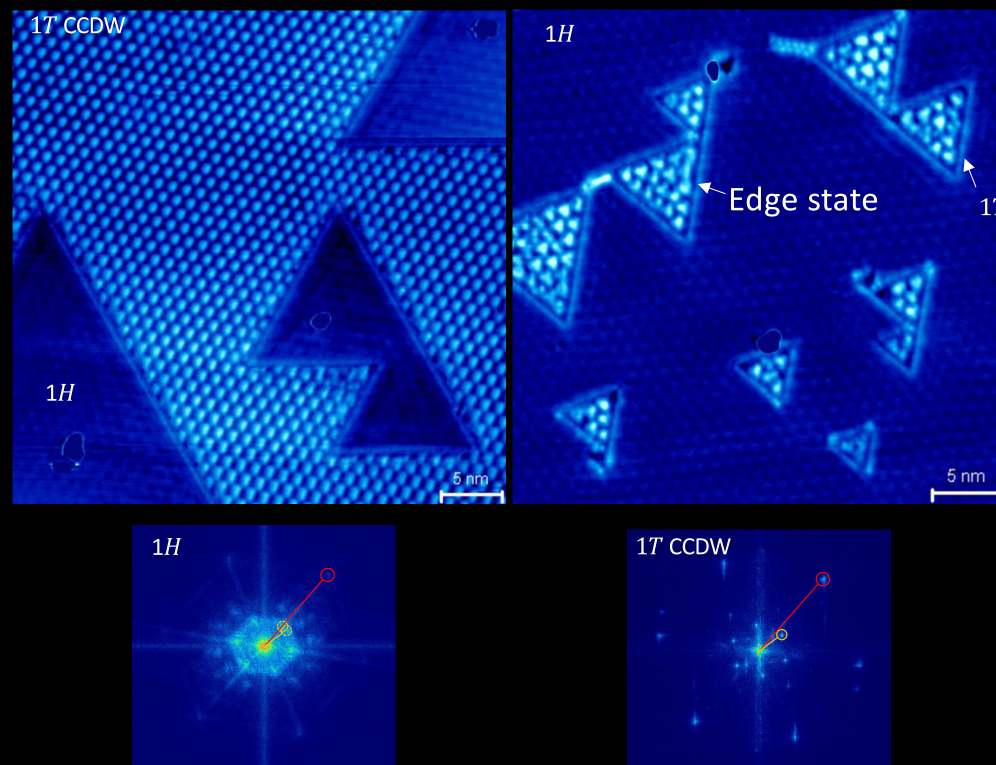

Ravnik et al., ACS *Applied Nano materials 2, 3743* (2019)

Setting up the Quantum billiard for confined electrons by temperature tuning

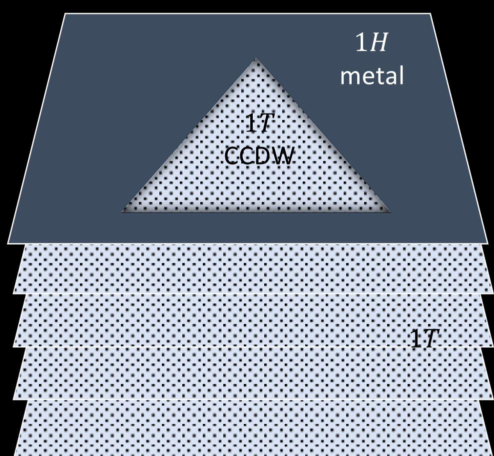

Superlattice structure

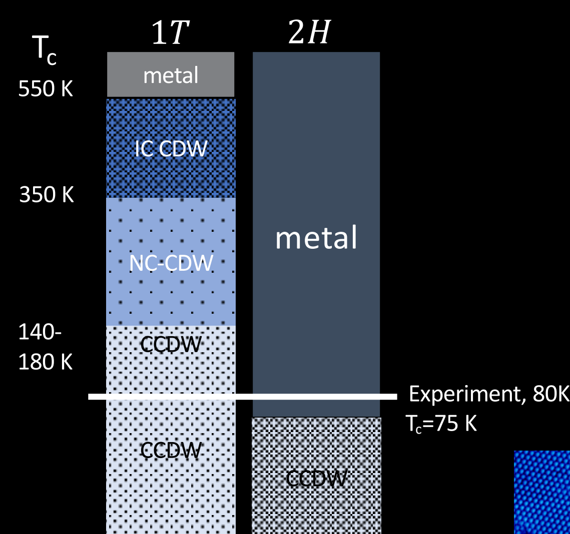

Phase diagram

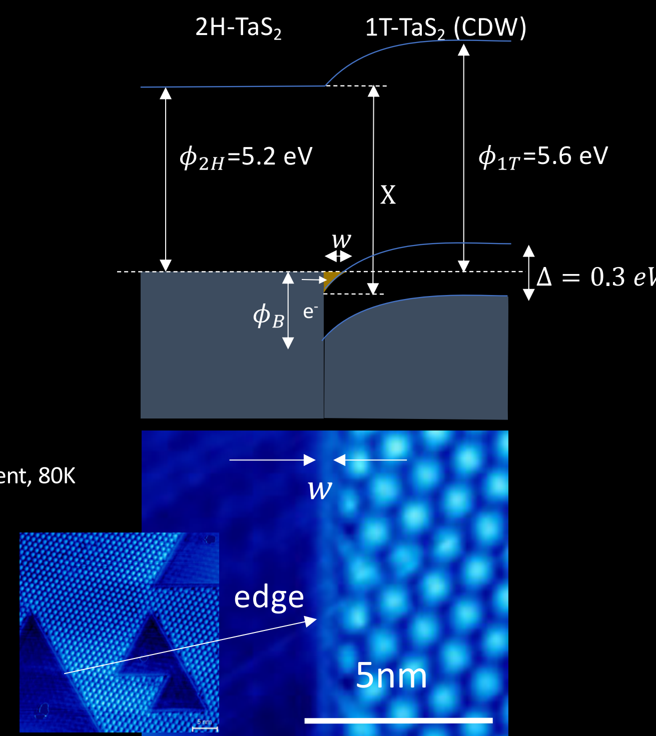

Energy level diagram

Classical billiard in an equilateral triangle

Classical trajectories

$(n > m)$

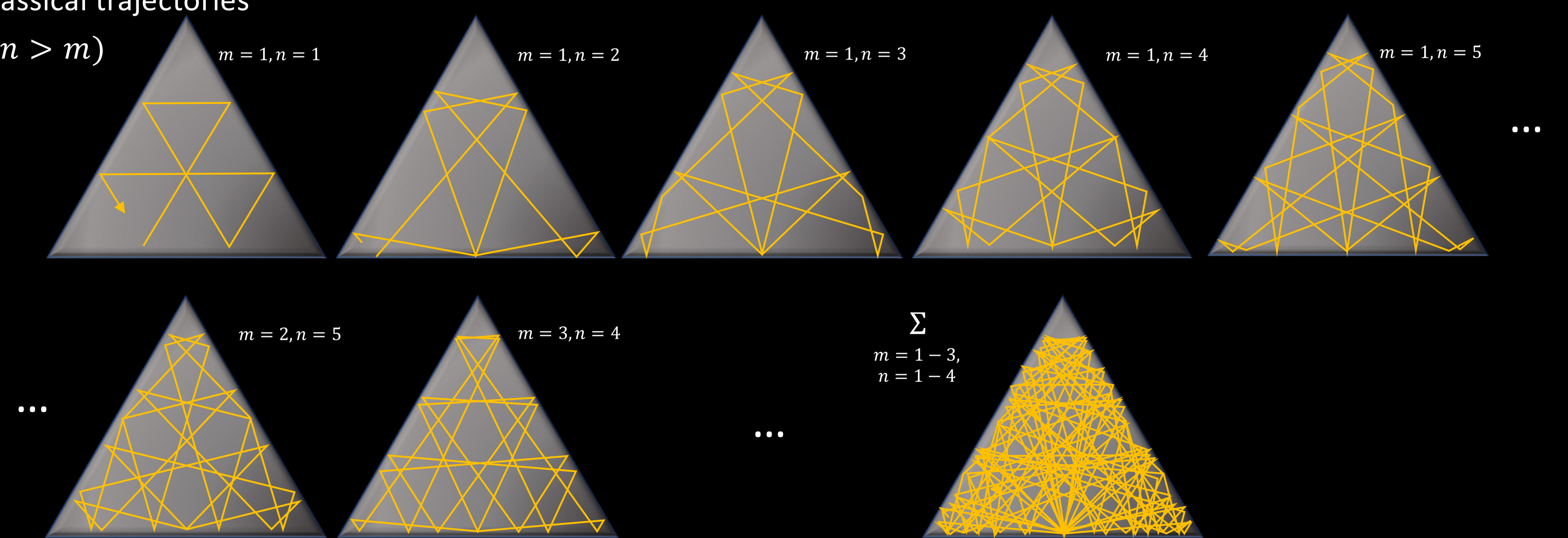

Panda et al., EPJ Plus (2019) 134, 3088

Quantum billiards in a perfect equilateral triangle

(Eigenstates of the Schrödinger equation)


nature COMMUNICATIONS

ARTICLE

https://doi.org/10.1038/s41467-021-24073-0 OPEN

Check for updates

Quantum billiards with correlated electrons confined in triangular transition metal dichalcogenide monolayer nanostructures

Jan Ravnik[1,2✉], Yevhenii Vaskivskyi[1], Jaka Vodeb[1,3], Polona Aupič[1], Igor Vaskivskyi[1,4], Denis Golež[3,5,6], Yaroslav Gerasimenko[4], Viktor Kabanov[1] & Dragan Mihailovic[1,4✉]

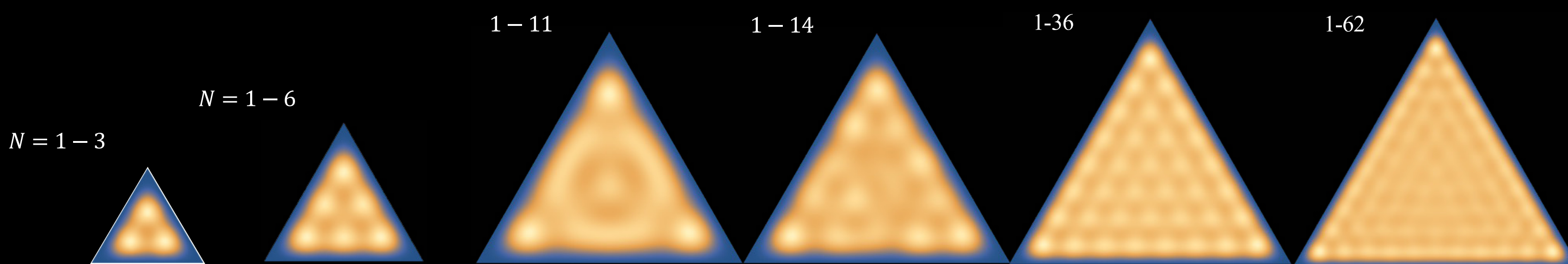

Plot of $\sum_N |\psi_i|^2$

Departure from a perfect equilateral triangle
→Quantum chaos

VOLUME 83, NUMBER 23 PHYSICAL REVIEW LETTERS 6 DECEMBER 1999

Mixing Property of Triangular Billiards

Giulio Casati[1] and Tomaž Prosen[2]

[1]*International Center for the Study of Dynamical Systems, Universita'degli Studi dell'Insub*
and Istituto Nazionale di Fisica della Materia and INFN, Unità di M

[2]*Physics Department, Faculty of Mathematics and Physics, University of Ljubljana, Jadran*

(Received 24 June 1999)

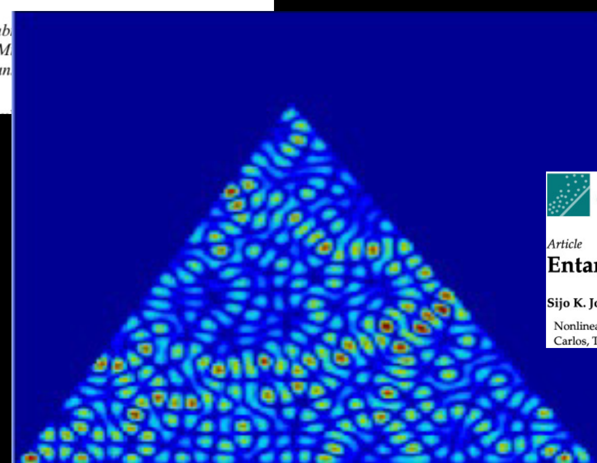

entropy MDPI

Article

Entanglement Entropy in a Triangular Billiard

Sijo K. Joseph * and Miguel A. F. Sanjuán

Nonlinear Dynamics, Chaos and Complex Systems Group, Departamento de Física, Universidad Rey Juan Carlos, Tulipán s/n, Móstoles, Madrid 28933, Spain; miguel.sanjuan@urjc.es

Wigner crystal confined within an E.T.

Confined charged lattice gas model with screened coulomb interaction (Vodeb et al, 2019) :

$$H = \sum_{i<j} V(i,j) n_i n_j$$

where

$$V(i,j) = V_0/r_{ij} \exp - \frac{r_{ij}}{r_s}$$

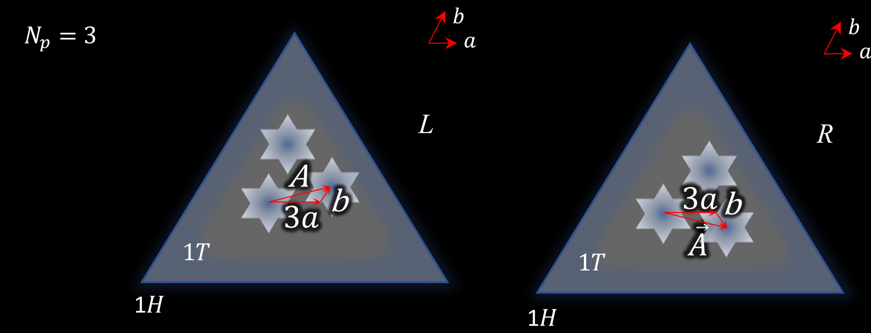

Filling patterns for different sizes of equilateral triangles:

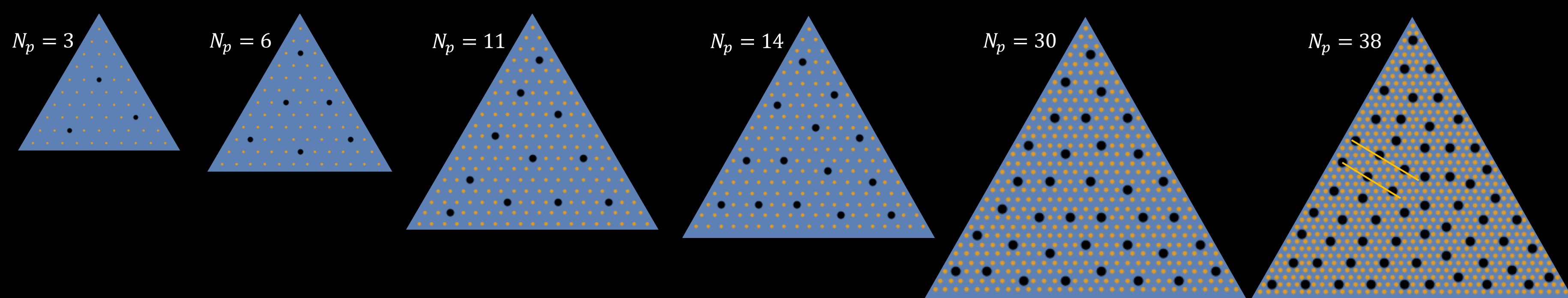

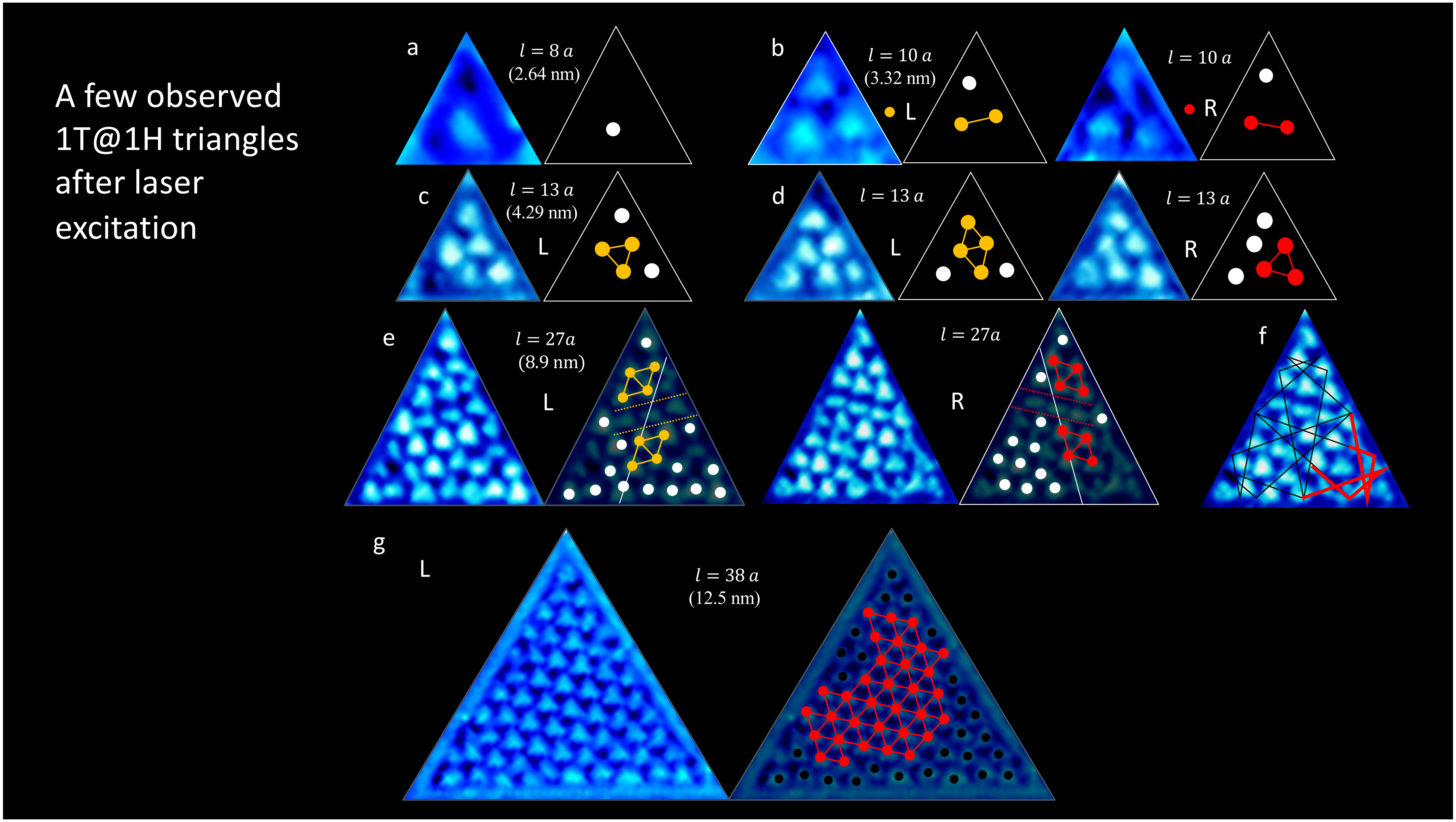
A few observed 1T@1H triangles after laser excitation
a
$l = 8\,a$
(2.64 nm)
b
$l = 10\,a$
(3.32 nm)
L
$l = 10\,a$
R
c
$l = 13\,a$
(4.29 nm)
L
d
$l = 13\,a$
L
$l = 13\,a$
R
e
$l = 27a$
(8.9 nm)
L
$l = 27a$
R
f
g
L
$l = 38\,a$
(12.5 nm)

Intertwined localized and itinerant electrons (a mixture of quantum billiards and CCDW)

The L and R triangles are created by the same laser pulse

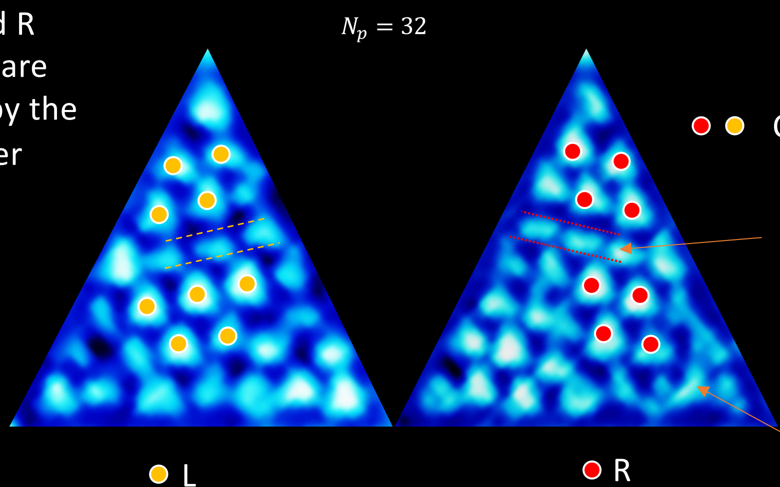

Correlation-localized electrons on a $\sqrt{13}\times\sqrt{13}$ lattice

Domain walls appear as a quasiparticle interference pattern

'Quantum scars' due to quasiparticle interference

STM image, $1T\Delta 1H$ triangles 80 K

Note: the itinerant particles are directly observed by the Quasiparticle interference (in mixed systems usually only the localized electron density is observed)

Interlayer effects: There is no preferential stacking between layers.

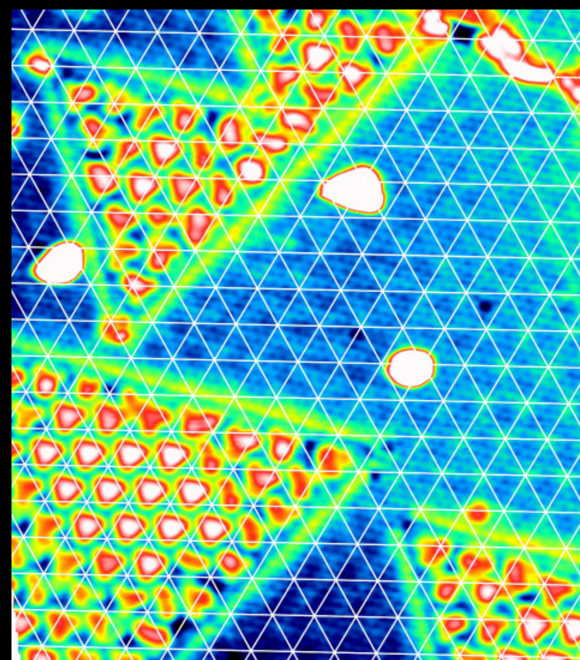

CCDW Layer
below in 1T-TaS_2
substrate

Edge effects, confined and unconfined electron states (STS measurements).

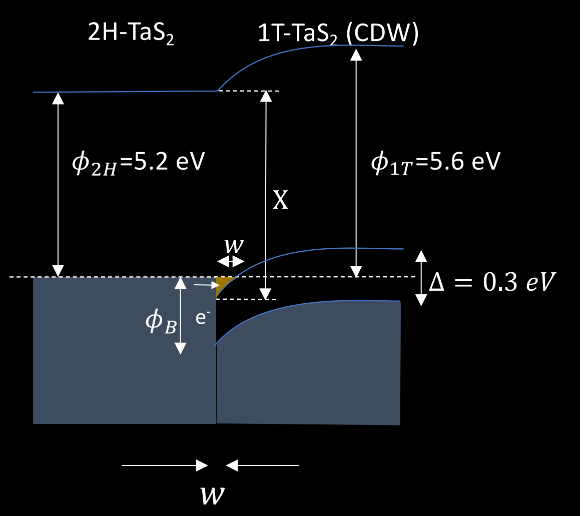

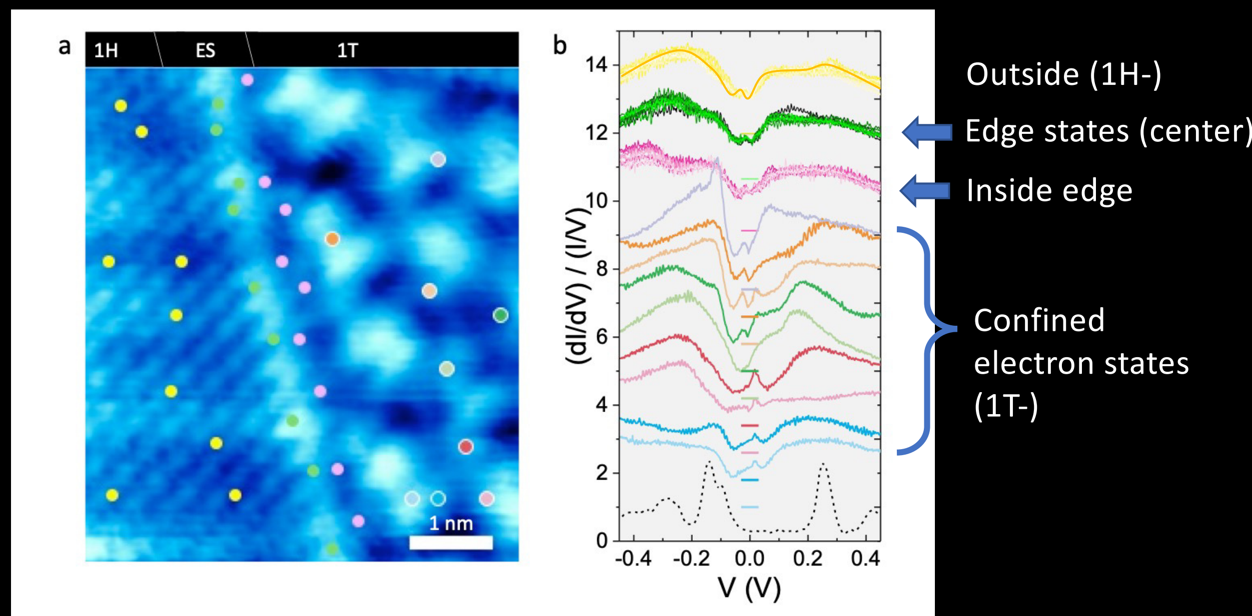

Carrier delocalization at incommensurate filling

Exact diagonalization calculation of electron delocalization (fully quantum)

$$H = -t \sum_{\langle i,j \rangle} c_i^{\dagger} c_j + \sum_{i \neq j} V(|i-j|)[n_i - \overline{n}][n_j - \overline{n}],$$

Delocalization parameter:

$$D = \sqrt{\Sigma_i [\langle n_i \rangle - \langle n_i \rangle^{t=0}]^2}$$

Incommensurate states ($N \neq 10$) are orders of magnitude more susceptible to delocalization than commensurate ones

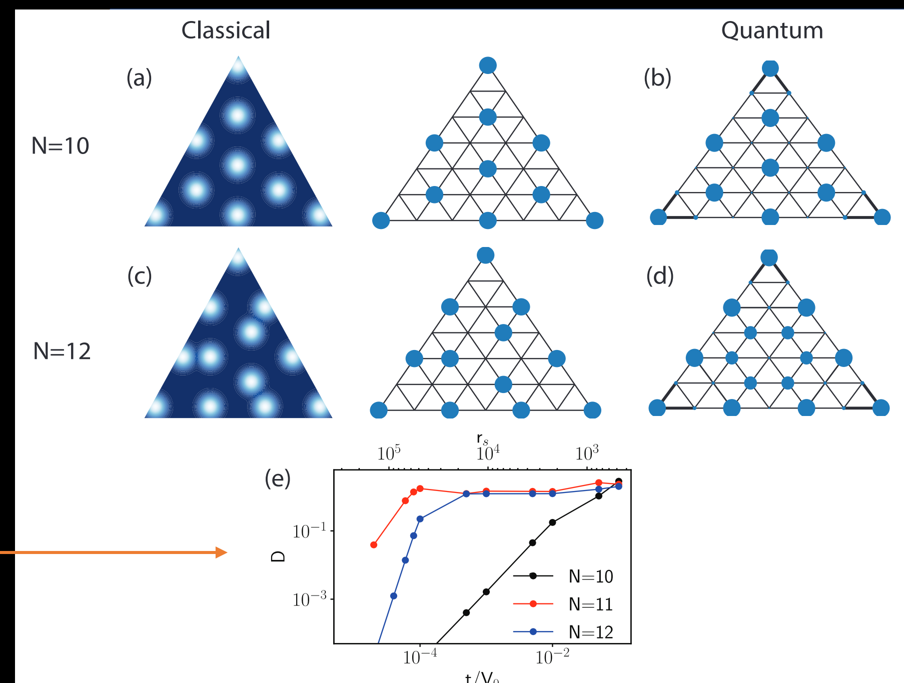

…Denis Golez, Nat. Comm., 2021

The different photoinduced states have very different transport (itinerant, localized)

Classical systems:
Kinematic constraints prevent lane change in a traffic jam

C state

H state

A state

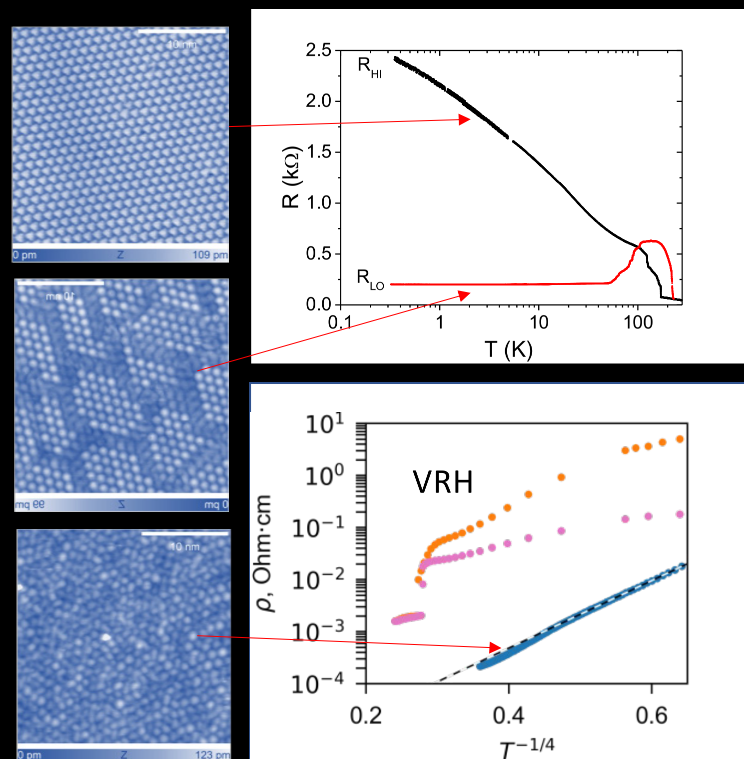

Tunnelling spectroscopy:

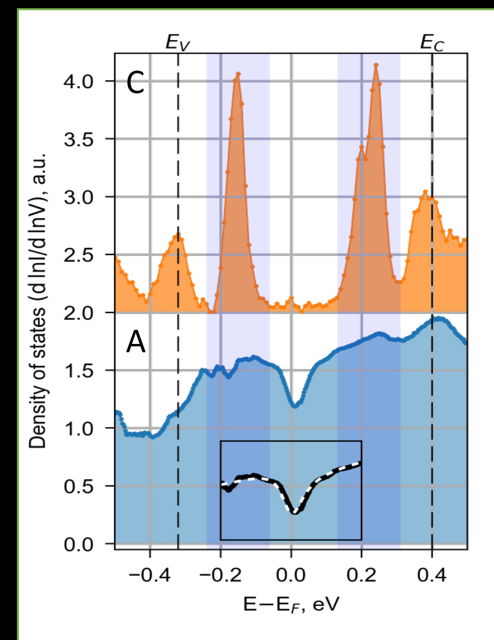

‘Nature Morte Vivante ’
by Salvador Dalí, 1956